Corticosteroid resistance is predetermined by early immune response dynamics at acute Graft-Versus-Host disease onset

One Sentence Summary (150 characters): Steroid-resistant acute graft versus host disease is set at disease onset as evidenced by specific transcriptomic signature, cell-to-cell crosstalk and trajectories.

Sophie Le Grand[1], Yannick Marie[2], Delphine Bouteiller[2], Emilie Robert[3], Régis Peffault de Latour[3,4], Gérard Socié[1,4], Nicolas Vallet[5]*, David Michonneau[1,4]*

Affiliations:

[1]INSERM UMR 1342, Translational Immunology in Immunotherapy and Hematology, Paris Cité University, F-75010, Paris, France

[2]Genotyping and Sequencing Facility, Paris Brain Institute-ICM, Hôpital de la Pitié-Salpêtrière, CNRS UMR 7225, INSERM U1127, Sorbonne Université UM75, CS21414, Paris, France.

[3]Cryostem Consortium.

[4]Hematology Transplantation, Saint Louis Hospital, Assistance Publique des Hôpitaux de Paris, 75010 Paris, France

[5]Hematology and Cell Therapy department, University Hospital of Tours, Inserm U1069 N2COx

*co-last authors

Corresponding author:

David Michonneau

Saint Louis hospital, hematology and transplantation

1 avenue Claude Vellefaux

75010 PARIS, FRANCE

david.michonneau@aphp.fr

Abstract

Corticosteroid-resistant acute graft versus host disease (SR-aGVHD) is the leading life-threatening complication following allogeneic hematopoietic stem cell transplantation. Novel therapeutics development is impeded by scares knowledge on biological pathways leading to steroid resistance at time of aGVHD diagnosis. To gain insight into our understanding on circulating immune cell subsets and functions at time of aGVHD and before steroid initiation, a single cell deep phenotyping and transcriptome analysis was performed on peripheral blood mononuclear cells from aGVHD patients before first line treatment, and from patients without aGVHD. We first explored immune cell subsets as a global signature, called immunotype. One immunotype enriched in monocytes expressing CD11b was associated with increased incidence of aGVHD (72% at day 100, log-rank p=0.005), but immunotypes were not associated with steroid sensitivity. Pathway analysis and inferred ligand/receptor interactions revealed major divergence between steroid sensitive and SR-aGVHD, including enrichment of TNFα activation in SR-GVHD, as well as TNF/TNFR, CCL3, CCL4 and IL18 signaling. Interferon α and γ pathways activation were decreased in SR-aGVHD patients. Finally, trajectory inferences within $CD8^+$ T cells evidenced specific transition during SR-aGVHD, from an early differentiated state to a highly activated and differentiated one, without slight differentiation across intermediate stages, involving specific gene signature during state transition. These findings provide evidence that corticosteroid resistance is an intrinsic mechanism already present at the onset of alloimmune response. This comprehensive overview of pathways underlying corticosteroid resistance highlights specific patterns that may serve as potential new therapeutic targets.

INTRODUCTION

Allogeneic hematopoietic stem cell transplantation (HSCT) is a major treatment for hematological malignancies. Its therapeutic effect is based on alloreactivity of donor T cells against tumor cells. However, donor T cells also react against healthy host cells, which may lead to graft-versus-host disease (GVHD). Acute GVHD (aGVHD) may involve skin, gut, or liver tissue. Its pathophysiology is initiated after tissue damage from high dose alkylating agent and radiation based-conditioning regimens leading to recognition of non-self-major and minor histocompatibility antigens (MHC and mHag(*1*)) and an alloreactive immune response, exacerbated by altered tissue repair mechanisms and microbiome dysbiosis(*2*). Despite first line treatment with prompt corticosteroid initiation(*3*, *4*), more than 40% of patients are steroid resistant (SR-aGVHD)(*5–7*). Steroid resistance is defined by an absence of clinical response after 7 days of standard dose of corticosteroids, a progressive disease after 3 days, progressive disease with new organ involvement or recurrence while steroids are stopped or tapered. Although ruxolitinib improves symptoms for 60% of SR-GVHD patients(*8*), their prognosis is very dismal(*3*, *9*, *10*).

While biomarkers were recently developed to improve aGVHD diagnosis and risk stratification(*11–15*), response to steroid is still unpredictable and biological mechanisms underlying steroid resistance remains only partly understood, even in the few experimental transplantation models of SR–GVHD described(*16–18*). In humans, specific whole gene expression analysis at diagnosis of lower intestinal acute SR-GVHD identified an increased repair-associated gene (amphiregulin and the aryl hydrocarbon receptor) and M2 macrophages pathways(*19*), suggesting that steroid resistance in not restricted to the T cells response as initially suspected. Indeed, neutrophils participate in tissue damage at GVHD onset and triggering, through reactive oxygen species production(*20*) and promote T cell expansion(*21*) and differentiation to Th17 cells(*22*, *23*). As corticosteroids increase neutrophils count and development, it has been hypothesized that corticosteroids may trigger a positive feedback loop between pathogenic T cells and neutrophils in SR-GVHD context(*24*).

Furthermore, neutrophil-predominant noncanonical inflammation pathways were recently identified in gut-SR-GVHD biopsies, notably ubiquitin specific peptidase 17–like family of genes(*25*). While gut microbiota's role has been extensively studied in GVHD, it is not well understood in SR-GVHD. Butyrate, a short-chain-fatty-acid product from *Blautia* bacteria is associated with better long terms outcomes in aGVHD(*26–28*), but one study found a negative association between butyrate production and SR-GVHD, due to the ability of butyrate to impair human colonic stem cells from recovering epithelial monolayer(*29*). Other studies identified SR-GVHD biomarkers such as IL-22(*16*), but with controversial potential(*30*, *31*). Most of these studies rely on murine models(*16–18*, *32*), and there is currently no clear overview of immune subsets associated with steroid resistance in human GVHD.

We hypothesize that reshaping of immune system might be initiated early in alloimmune responses, therefore predisposing to corticosteroids refractoriness. To describe immune subsets and their respective function, cellular indexing of transcriptomes and epitopes sequencing (CITE-Seq) was performed on peripheral blood mononuclear cells (PBMC) samples collected at the onset of aGVHD before first line treatment, or in patient without GVHD at day 100 after HSCT. Whole landscape of circulating immune cells at early onset of aGVHD and its association with GVHD severity was uncovered. Deep analysis of transcriptomic profiles revealed that steroid resistance is an intrinsic property of the immune response, characterized by specific enriched biological pathways, specific cell-to-cell crosstalk through ligand-receptor interactions and a specific immune trajectory involving most immune subsets. Altogether, our results highlight that steroid-resistant GVHD is an early characteristic of allo-immune response before any immunosuppressive treatment and pave the way to more targeted first-line therapy to improve allogeneic HSCT outcomes.

RESULTS

Cohort's characteristics

Samples from 53 patients were retrieved from the prospective CRYOSTEM multicenter collection. PBMC were collected before corticosteroids initiation for patients diagnosed with aGVHD, and at day 100 post allo-HSCT for non-GVHD patients. Hematological malignancies, HSCT procedure and clinical characteristics were balanced between groups (**Table S1)**. Among the 21 aGVHD patients, 16 (76%) were steroid sensitive (SS-GVHD) and 5 (24%) were steroid refractory (SR-GVHD) (**Figure 1A**). For validation and control purposes, 6 samples from healthy blood donor were used. After samples preparation for CITE-seq experiments, sequencing, quality control filtering and data processing acquisition, more than 300,000 single cells were available for immune profiling and transcriptome analysis (**Figure 1B**). Unsupervised clustering resulted in the identification of 40 immune cell subsets (**Figure 1C and S1**), characterized by their surface antigens expression (**Figure 1D**).

Immune signature and increased proliferation associate with aGVHD onset but not with response to steroids

Compared to non-aGVHD patients, classical monocytes CD73^{+} were significantly enriched in aGVHD patients, whereas NK and B cell subsets were significantly decreased (**Figure 1E**). To encompass the compositional structure of immune subsets frequencies, principal coordinates analysis (PCoA) was used. Four distinct immune clusters were identified, thereafter called immunotypes (**Figure 2A**). aGVHD patient's distribution was significantly different among immunotypes (p=0.001, **Table S2**, **Figure 2B**), as well as the GVHD cumulative incidence (**Figure 2C,** Immunotype 4 GVHD incidence = 72% at day 100, *vs* immunotype 1 = 55%, *vs* immunotype 2 = 38%, *vs* immunotype 4 = 0%, global log-rank p=0.005). GVHD-free and relapse-free survival (GRFS) was significantly associated with immunotypes (p=0.0048, **Figure S2**), however there were no significant differences in non-relapse mortality and

cumulative incidence of relapse (**Figure S2**). Association with other clinical variables is depicted in **Figure S3**.

Immunotype 1 and 4 included a large number of patients with aGVHD (**Figure 2B–C**), and were characterized by an overall reduction in immune cell heterogeneity, illustrated with an imbalanced immune subsets representation (**Figure 2D**). Especially, immunotypes 1 and 4 presented a high display of classical monocytes CD11b^{bright} (IgM^{+} or IgM^{-}) compared to other immunotypes. Immunotype 2 and 3 were characterized by a balanced distribution across different immune cell populations, and a lower classical monocytes CD11b^{bright} cells representation. Remarkably, immunotype 3 was characterized by an absence of patients with aGVHD, a decrease in classical monocytes CD11b^{bright} and in other monocytes populations, whereas effector T CD4^{+} and CD8^{+} were predominantly increased.

To further investigate whether the over-representation may encompass a high cell division rate at time of aGVHD diagnosis, we determined cell cycle phase scoring within each immune cell population. Immune populations were predominantly in S phase (**Figure 3A**), reflecting increase cell proliferation at aGVHD onset.

No significant differences among immune cells abundances, immunotypes and cell-cycle scoring was observed with respect to corticosteroid resistance (**Figure 2B**, **Table S2, Figure S4 and S5**). In summary, immune cells subset clearly identified patients without GVHD but hardly discriminated SS and SR-GVHD. We thus hypothesized that cell intrinsic biological functions may predispose to SR-GVHD.

Steroid resistance is associated with enrichment of TNFα and metabolic pathways at aGVHD onset

We first considered the biological pathways enriched at the onset of aGVHD by comparison with patients without GVHD (**Figure S6**). When considering aGVHD as a whole,

we observe overactivation of IFNα and γ pathways in all immune cells, and a decrease in TNFα signaling, especially in $CD8^+$ T cells and myeloid cells.

To study which biological process may correlate with subsequent SS- or SR-aGVHD, we then performed a second enrichment analysis in patients with SS- or SR-aGVHD. Compared to SS-aGVHD, inflammation pathways were enriched in SR-aGVHD patients within all immune cells; particularly TNFα and hypoxia pathways (**Figure 3B**). STAT5 and MTORC pathways were particularly upregulated in exhausted effector memory $CD4^+$ and $CD8^+$ T cells, in naïve $CD8^+$ T cells and in dendritic immune cells. The IL6/JAK STAT pathway was also highly enriched in naive $CD8^+$ T cells and classical $CD11b^{bright}$ monocytes.

Genes associated with metabolism pathways were overexpressed, especially oxidative phosphorylation in naïve $CD4^+$ T cells, double negative T cells and myeloid cells. Conversely, there was a decreased activation of the IFNα and γ responses within all immune subsets, except NK cells.

Cell to cell crosstalk during SR-GVHD specifically involves IL1, CCL3, CCL4, TNFα and IL18 signaling

To address whether cell biological processes involved in SR-aGVHD may be involved in cell-to-cell interactions leading to early steroid-resistance, we examined intercellular communication using a computational inferring method(*33*). When focusing on $CD8^+$ T cells as receiver, 20 ligands were identified as prioritized ligands, and their expression on sender cells is shown in **Figure 4A**. IL1B, CCL3 and CCL4 ligands were particularly overexpressed in SR-aGVHD condition (**Figure 4B**). Regulatory potential of each ligand with predicted targets genes in shown in **Figure 4C**.

Predicted ligands and targets interaction were then analyzed for CD4 regulatory T cells (**Figure S7A**), NK cells (**Figure S7B**), $CD4^+$T cells (**Figure S8A**), and double negative T cells (**Figure S8B**). An overview of all these interactions is depicted as a circus plot (**Figure 4D**) based on biologically confirmed interactions previously designated as *bona fide* interactions

(**Figure S9A**). TNF ligands-to-cell signaling appeared to be overexpressed in most sender cells in SR-aGVHD patients, as well as CCL3, CCL4 and IL18. ADAM17, which is involved in TNF activation(*34*), was overexpressed in all senders and interacted with TNFR, ITGAL and ITGB2 receptors. Interestingly, IFN/IFNR interactions was enhanced across all receivers in SR-aGVHD but absent in SS-aGVHD.

Conversely, when comparing patients with aGVHD to those without aGVHD, immune cells crosstalk appeared different to that disclosed in the SS- and SR–aGVHD setting (**Figure S9B**). Consistent with enrichment analysis, TNF/TNF-R interaction was decreased among DN T cells, NK cells and T regulatory lymphocytes. TGFB1/TGFBR interactions, which are considered as being associated with an immunoregulatory role, were significantly increased in patient with no aGVHD compared to aGVHD patients. Especially within $CD8^+$ T cells, as well as BTLA/TNFRSF14 interaction, a pathway previously identified in animal models as a regulator of alloimmune response(*35*, *36*).

Specific trajectories were associated with SR-GVHD

As biological processes and cell-to-cell interactions targeting $CD8^+$ T cell were associated with SR-aGVHD, we hypothesized that immune cells subsets from SR-aGVHD and SS-aGVHD patients may exert specific $CD8^+$ T cell trajectories. To address this hypothesis, trajectories within $CD8^+$ T cell were defined on a new cell clustering based on mRNA expression (**Figure S10**). Two trajectories were identified: (i) lineage 1 described in **Figure 5A-B** and (ii) lineage 2 described in **Figure S11**.

Frequency of cells in lineage 1 slightly increased over pseudotime in SS-aGVHD patients through multiple transition states starting from naïve double positive T cell (cluster 27) to effector memory $CD8^+$ T cell expressing ICOS (cluster 2) **(Figure 5A-B).** By contrast, SR-aGVHD patients were characterized by a direct transition with very few cells in the transition subsets (cluster 15, 9 and 10), most immune subset being grouped in cluster 27 at early pseudotime or in cluster 2 in late pseudotime. The same pattern was observed in the

second $CD8^+$ T cell trajectory, with a transition from naïve double positive T cell (cluster 27) to $CD8^+$ TEMRA cells expressing ICOS and PD1 (cluster 25) (**Figure S11A-B**).

To highlight different gene expression pattern in SS-aGVHD and SR-aGVHD we first studied individual genes whose expression varied significantly along pseudotime and across transition state (**Figure 5C, S11C, Table S3-S10**). Among the most significant genes involved in transition states, we identified CCL4, CCL5, IFI6, LAG3, and TIGIT (**Table S11 and S12**). SR-aGVHD patients exhibited earlier and higher CCL4 and LAG3 expression in pseudotime (**Figure 5D and S11D**). Consistently with pathway enrichment analysis, IFI6 expression, indicative of IFNα activation, was higher in SS-aGVHD patients, particularly in early-differentiated $CD8^+$ T cells.

To study overall biological processes, we used hierarchical clustering to identify modules of correlated gene among the top 500 expressed gene along pseudotime lineages. This approach identified 5 modules of genes involved in cell-to-cell transition (**Figure 5C**). Over-representation analysis (ORA) from Gene Ontology knowledgebase within each cell subset highlighted the main biological pathways involved at each transition state (**Figure 5E**). SR-aGVHD was notably associated with an early enrichment of pathways associated with cell activation and high transcriptional and translational activity in naïve double positive T cell (**Figure S11E**). A detailed analysis of pathways enriched in each module revealed striking differences in the dynamics of T cell activation during SR-GVHD (trajectory 1 in **Figure S12 and S13,** and trajectory 2 in **Figure S14 and S15**).

Overall, these results reveal that even before starting corticosteroids, aGVHD is already characterized by different trajectories and pattern of gene activation between transition states, that can define a specific dynamic of alloimmune response during steroid resistance.

DISCUSSION

Despite recent advances in the management of aGVHD, steroid-resistant treatment remains a challenge. This study is the first to describe immune subsets and transcriptional profiles in human at time of aGVHD. Early identification of patients at risk of developing steroid resistance is crucial for rapid and tailored therapeutic intervention. Up to now, a comprehensive understanding of the circulating immune cells mechanisms associated with steroid resistance has not been addressed. Our results highlight that steroid resistance is characterized at the onset of aGVHD, by a specific transcriptomic profile that reveal biological pathways, cell-to-cell interactions and trajectories that differ from steroid sensitive patients.

Immunotypes and cell cycle scoring enabled the identification of specific patterns associated with aGVHD compared to non-aGVHD patients. Immunotype 4, characterized by poor immune cell diversity and by classical $CD11^+$ monocytes abundance was associated with worsened aGVHD free survival. This observation is consistent with previous studies identifying monocytes and macrophages as fully parts of the immune response at aGVHD onset (*19*, *37*–*40*).

However, cell subsets distribution did not allow to distinguish SS- and SR-aGVHD. When focusing on immune cells functions rather than distinct phenotypes, we found specific patterns associated with SR-GVHD, especially higher TNFα pathway activation. This was strengthened with inferred interaction analyses which revealed an increased TNF/TNFR interaction, notably in $CD8^+$ T cells. Although this *in silico* prediction would need to be confirmed *in vivo*, these results might suggest that early anti-TNF therapies could be beneficial in patients with the corticosteroid resistance profile we described herein. This is supported by previous clinical phase 2 trial testing a combined therapy of anti-TNF and corticosteroids, with increased response rate (69% vs 33%; $P < 0.001$) without increased infections risk(*41*).

Interferon have been described for their crucial role in aGVHD development (*42*, *43*). We found that IFNα and γ pathways were activated at time of aGVHD and before corticosteroid treatment. Unexpectedly, SR-aGVHD was associated with lower activation of IFNα and γ

pathways, and INFG/IFNGR interactions were increased in SR-aGVHD setting. This suggests that the IFN signals might be blocked after receptor activation. Moreover, IFI6, a protein-coding gene for IFNα, is expressed earlier and at higher levels during T cell differentiation in SS-aGVHD.

Cross-talk analysis revealed numerous interactions specifically associated with corticosteroids resistance, especially with cytokines/cytokines-receptors such as IL18, CCL4, CCL5. Increased in CCL4 and CCL5 interactions within $CD8^+$ T cells populations suggest the recruitment of effectors to inflammatory sites. IL18 is a proinflammatory cytokine which can promote interferon γ production(*44*), and was already described as an important player in aGVHD pathogenesis(*45*), as serum levels in post-HSCT patients were associated with aGVHD severity ($r = 0.861$, $P < 0.001$)(*45*).

Finally, trajectory inferences highlighted specific layouts associated with SR-aGVHD. Cells were particularly abundant in low and high pseudotime in SR-GVHD patients, while there was a progressive increase along pseudotime in SS-GVHD patients. It suggests that cells in SR-GVHD patients quickly differentiate to terminally activated states. This was consistent with, higher and earlier gene expression of LAG3 and TIGIT in SR-GVHD patients. Consistent with results from cell-cell interactions analysis, CCL4 and CCL5 were expressed at higher levels and earlier in SR-GVHD patients, as already described in animal model(*46*).

Because samples were collected before cortico-steroid initiation, our work sheds light on early signature pathways leading to corticosteroid resistance. These pathways appeared distinct from those involved in the general inflammatory response of acute GVHD and could be targeted as early as steroid initiation. Transcriptomic analysis offered a powerful approach to unravel immune cells functionality, combined with precise phenotypic population identification, allowing for the identification of cellular heterogeneity in SR-GVHD immune response. The complexity of the immune response in the context of GVHD was already investigated at the single cell level, through T cell subset analysis following TCR clonotype mapping(*47*). This elegant approach, though limited by patient's number, revealed that each

patient possessed a highly intricate repertoire, with different tissues exhibiting distinct clonal populations, varying degrees of repertoire overlap between sites, and diverse numbers of dominant clones shared across multiple tissues(*47*). Another study investigated the role of Friend virus leukemia integration 1 in aGVHD context and found that this virus was able to activate and differentiate alloreactive CD4+ T cell(*48*).

Our study offers new insights into the immune complexity, presenting a broader perspective of the immune response. Our findings are partly limited by the use of models that would require additional validation *in vivo*. Moreover, additional studies focusing on immune infiltrates in target organs of GvHD would certainly help to complete our understanding of acute GVHD pathophysiology, and especially of mechanisms associated with corticosteroid resistance.

Overall, these findings provide evidence that corticosteroid resistance is an intrinsic mechanism already present at the onset of alloimmune response, highlighting specific patterns that may serve as potential new therapeutic targets.

MATERIALS AND METHODS

Cohort

This study was conducted with samples from patients and healthy donors. Patients were included in the CRYSOTEM cohort after validation by the scientific committee (study number CS-1801). Cryostem consortium was approved by IRB Sud-Mediterranée 1 (reference number AC-2011-1420) and the Commission National Informatique et Liberté for data protection (reference number nz70243374i n°912120). All patients gave their written consent for clinical research and sample collection. This non-interventional research study with no additional clinical procedure was carried out in accordance with the Declaration of Helsinki. Data analyses were carried out using an anonymised database. Healthy donor's PBMC were

isolated from residual blood after apheresis provided by Etablissement Français du Sang (18/EFS/032).

CITE Seq experiment

After thawing cells in a 50% fetal calf serum (FCS)/RPMI medium, 10x Genomics Feature Barcoding recommendations were followed. Cells were washed twice using a 10 mL solution of the same media. 500 000 cells were transferred in a 0.04% PBS/bovine serum albumin (BSA) medium and washed. Cells were then suspended in a 1% PBS/BSA solution before incubation with oligonucleotide-coupled antibodies TotalSeq-B (panel described in **Table S13**) for 60 min on ice. Cells were washed 4 times (4°C, RCF 300, 5 minutes) and suspended in order to obtain a concentration of 1 000 cells/µL. 10 000 cells were subjected in Gel Bead Emulsion using Chromium 10x Genomics controller, according to manufacturer guidelines. Chromium™ Next GEM Single Cell 3' Kit v3.1 (10X Genomics, cat. 1000268) and 3' Feature Barcode Kit (10X Genomics, cat. 1000262) were used to prepare reagents.

To perform single cell RNA sequencing after cDNA amplification, the concentration of each sample was measured using Tapestation 2200 (Agilent). To prepare the cDNA libraries for 10x Genomics Chromium controller, we used the single-cell 3′ v3.1 kit (Dual Index) with Feature Barcode technology for Cell Surface Protein, following manufacturer guidelines. QC libraries were performed using Tapestation 2200 (Agilent). Libraries were equimolar pooled to obtain at least 20 000 read pairs per cell and 5 000 read pairs for feature barcode part after sequencing on Illumina Novaseq 6000 (100 cycles cartridge). The input number of cells was estimated at 10 000 cells/samples. FASTQ files were obtained with bcl2fastq (Illumina).

Data quality control

Alignment, filtering, barcode counting, UMI counting were performed with count function from 10x Genomics Cell Ranger (version 6.0) using GRCh38 genome assembly as reference data.

Then aggr function was used to aggregate results without normalization. A R environment (version 4.3.1) was subsequently used for the following analyses. Briefly, using Seurat R package(*49*), dead cells were excluded if mitochondrial RNA was above 18%; singlet were identified as droplets with RNA feature between 200 and 4 700; RNA and cell surface antigen counts were normalized and scaled using Seurat R package normalisation and scaling function for linear transformation. 2 000 highly variable RNA features were identified.

Immune cell clusterization

Using a principal component analysis method on the scaled data, cells were clustered according to cell surface antigen expression. We used UMAP for cluster visualization. Seurat R package was then used to calculate cell cycle phase based on canonical transcripts, and regressing these out of the data.

Enrichment pathways analysis

Fast preranked gene set enrichment analysis was performed using FGSEA package(*50*) with "hallmarks" gene reference data set from Molecular signature database(*51*). Pathways were compared between GVHD and non-GVHD patients, and between SR-GVHD and SS-GVHD patients. Gene expression comparison between GVHD and non GVHD patients, and between SS- and SR-GVHD patients was provided by differential expression analysis. Enrichment scores associated with adjusted p-value < 0.05 were selected for dot plot visualisation.

NicheNet Analysis

Ligand-receptors interaction was computed using NicheNet package(*33*). Sender cells were identified as myeloid cells, B cells, $CD4^+$ conventional T cells and regulatory T cells. Receiver cells were identified as $CD4^+$ and $CD8^+$ T lymphocytes, NK cells and regulatory T cells. Three pooled human gene expression data of interacting cells(*52–54*) were used as input and

combined with a prior model that integrates existing knowledge on ligand-to-target signalling paths to perform ligand activity analyses. Circos plot visualisation integrated *bona fide* interactions of each receiver, and increased or decreased interactions were integrated from "ligand differential expression heatmap" NicheNet output.

Trajectory inferences

Trajectory were based on RNA expression clusterisation (**Figure S10**). SingleCellExperiment object was subset by immune populations (CD8+ T cells, CD4+ T cells, NK cells, B cells and myeloid cells) before pseudotime calculation using slingshot package(*55*). TradSeq package was then use for downstream analysis(*56*). Briefly, associationTest R function evidenced genes whose expression is associated with pseudotime. Since pseudotime is a continuous value, it was divided into 50 categories for graphical representation with heatmap. Only the 500 most expressed gene in SS- and SR-GVHD were selected for heatmap visualization (**Table S3-S6**). Each point on X axis corresponded to a cell cluster with similar pseudotimes. The immune populations represented on top of the heatmap corresponded to the immune cell population most abundantly represented within the cell cluster (**Table S7-S10**). Gene markers specific to low pseudotime or high pseudotime were found thanks to starVsEndTest command. Expression along pseudotime in each condition was plotted for four genes from the top 100 starVsEndTest output **(Figure 5, Tables S11 and S12)**. To explore the pathways associated with gene expression of the top 500 most expressed genes along pseudotime from each of the 5 modules of the heatmap, we used over-representation analysis using enrichGO command from clusterProfiler R package(*57*). Only pathways associated with adjusted pval < 0.05 from "molecular functions" and "biological process" of the Gene Ontology knowledgbase(*58*, *59*) were selected for dot plots visualization.

List of Supplementary Materials

Fig. S1: Immune populations in each group of patients

Fig. S2: Immunotype survival analysis

Fig. S3: Immunotype and clinical variables

Fig. S4: Immune cell abundance in SS- and SR-GVHD patients

Fig. S5: Cell cycle in SS- and SR-GVHD patients

Fig. S6: Pathways enrichment in aGVHD patients

Fig. S7: Interactions combined plots in regulatory T cells and NK cells

Fig. S8: Interactions combined plots in $CD4^+$ T cells and double negative T cells

Fig. S9: Bona fide interactions in all receivers

Fig. S10: Clustering based on RNA expression

Fig. S11: $CD8^+$ T cells lineage 2 trajectory analysis

Fig. S12: Over representation analysis in lineage 1 SR-GVHD patients

Fig. S13: Over representation analysis in lineage 1 SS-GVHD patients

Fig. S14: Over representation analysis in lineage 2 SR-GVHD patients

Fig. S15: Over representation analysis in lineage 2 SS-GVHD patients

Table S1: Patients' characteristics

Table S2: Characteristics according to immunotypes

Table S3: Top 500 genes expression matrix in lineage 1 SR-GVHD patients

Table S4: Top 500 genes expression matrix in lineage 1 SS-GVHD patients

Table S5: Top 500 genes expression matrix in lineage 2 SR-GVHD patients

Table S6: Top 500 genes expression matrix in lineage 2 SS-GVHD patients

Table S7: Immune population mostly represented along pseudotimes in lineage 1 SR-GVHD patients

Table S8: Immune population mostly represented along pseudotimes in lineage 1 SS-GVHD patients

Table S9: Immune population mostly represented along pseudotimes in lineage 1 2 SR-GVHD patients

Table S10: Immune population mostly represented along pseudotimes in lineage 2 SS-GVHD patients

Table S11: StartvsEnd output in lineage 1

Table S12: StartvsEnd output in lineage 2

Table S13: Total-Seq-B antibody panel

REFERENCES

1. N. Cieri, N. Hookeri, K. Stromhaug, L. Li, J. Keating, P. Díaz-Fernández, V. Gómez-García de Soria, J. Stevens, R. Kfuri-Rubens, Y. Shao, K. A. Kooshesh, K. Powell, H. Ji, G. M. Hernandez, J. Abelin, S. Klaeger, C. Forman, K. R. Clauser, S. Sarkizova, D. A. Braun, L. Penter, H. T. Kim, W. J. Lane, G. Oliveira, L. S. Kean, S. Li, K. J. Livak, S. A. Carr, D. B. Keskin, C. Muñoz-Calleja, V. T. Ho, J. Ritz, R. J. Soiffer, D. Neuberg, C. Stewart, G. Getz, C. J. Wu, Systematic identification of minor histocompatibility antigens predicts outcomes of allogeneic hematopoietic cell transplantation. *Nat Biotechnol*, 1–12 (2024).
2. R. Zeiser, B. R. Blazar, Acute Graft-versus-Host Disease — Biologic Process, Prevention, and Therapy. *N Engl J Med* **377**, 2167–2179 (2017).
3. A. C. Harris, R. Young, S. Devine, W. J. Hogan, F. Ayuk, U. Bunworasate, C. Chanswangphuwana, Y. A. Efebera, E. Holler, M. Litzow, R. Ordemann, M. Qayed, A. S. Renteria, R. Reshef, M. Wölfl, Y.-B. Chen, S. Goldstein, M. Jagasia, F. Locatelli, S. Mielke, D. Porter, T. Schechter, Z. Shekhovtsova, J. L. M. Ferrara, J. E. Levine, International, Multicenter Standardization of Acute Graft-versus-Host Disease Clinical Data Collection: A Report from the Mount Sinai Acute GVHD International Consortium. *Biol Blood Marrow Transplant* **22**, 4–10 (2016).
4. L. Axt, A. Naumann, J. Toennies, S. P. Haen, W. Vogel, D. Schneidawind, S. Wirths, R. Moehle, C. Faul, L. Kanz, S. Axt, W. A. Bethge, Retrospective single center analysis of outcome, risk factors and therapy in steroid refractory graft-versus-host disease after allogeneic hematopoietic cell transplantation. *Bone Marrow Transplant* **54**, 1805–1814 (2019).
5. O. Penack, M. Marchetti, M. Aljurf, M. Arat, F. Bonifazi, R. F. Duarte, S. Giebel, H. Greinix, M. D. Hazenberg, N. Kröger, S. Mielke, M. Mohty, A. Nagler, J. Passweg, F. Patriarca, T. Ruutu, H. Schoemans, C. Solano, R. Vrhovac, D. Wolff, R. Zeiser, A. Sureda, Z. Peric, Prophylaxis and management of graft-versus-host disease after stem-cell transplantation

for haematological malignancies: updated consensus recommendations of the European Society for Blood and Marrow Transplantation. *Lancet Haematol* **11**, e147–e159 (2024).

6. P. J. Martin, J. D. Rizzo, J. R. Wingard, K. Ballen, P. T. Curtin, C. Cutler, M. R. Litzow, Y. Nieto, B. N. Savani, J. R. Schriber, P. J. Shaughnessy, D. A. Wall, P. A. Carpenter, First- and second-line systemic treatment of acute graft-versus-host disease: recommendations of the American Society of Blood and Marrow Transplantation. *Biol Blood Marrow Transplant* **18**, 1150–1163 (2012).
7. J. R. Westin, R. M. Saliba, M. De Lima, A. Alousi, C. Hosing, M. H. Qazilbash, I. F. Khouri, E. J. Shpall, P. Anderlini, G. Rondon, B. S. Andersson, R. Champlin, D. R. Couriel, Steroid-Refractory Acute GVHD: Predictors and Outcomes. *Adv Hematol* **2011**, 601953 (2011).
8. R. Zeiser, N. von Bubnoff, J. Butler, M. Mohty, D. Niederwieser, R. Or, J. Szer, E. M. Wagner, T. Zuckerman, B. Mahuzier, J. Xu, C. Wilke, K. K. Gandhi, G. Socié, REACH2 Trial Group, Ruxolitinib for Glucocorticoid-Refractory Acute Graft-versus-Host Disease. *N Engl J Med* **382**, 1800–1810 (2020).
9. P. J. Martin, G. Schoch, L. Fisher, V. Byers, C. Anasetti, F. R. Appelbaum, P. G. Beatty, K. Doney, G. B. McDonald, J. E. Sanders, A retrospective analysis of therapy for acute graft-versus-host disease: initial treatment. *Blood* **76**, 1464–1472 (1990).
10. R. Zeiser, N. von Bubnoff, J. Butler, M. Mohty, D. Niederwieser, R. Or, J. Szer, E. M. Wagner, T. Zuckerman, B. Mahuzier, J. Xu, C. Wilke, K. K. Gandhi, G. Socié, Ruxolitinib for Glucocorticoid-Refractory Acute Graft-versus-Host Disease. *N Engl J Med* **382**, 1800–1810 (2020).
11. J. L. M. Ferrara, A. C. Harris, J. K. Greenson, T. M. Braun, E. Holler, T. Teshima, J. E. Levine, S. W. J. Choi, E. Huber, K. Landfried, K. Akashi, M. Vander Lugt, P. Reddy, A. Chin, Q. Zhang, S. Hanash, S. Paczesny, Regenerating islet-derived 3-alpha is a biomarker of gastrointestinal graft-versus-host disease. *Blood* **118**, 6702–6708 (2011).
12. M. T. Vander Lugt, T. M. Braun, S. Hanash, J. Ritz, V. T. Ho, J. H. Antin, Q. Zhang, C.-H. Wong, H. Wang, A. Chin, A. Gomez, A. C. Harris, J. E. Levine, S. W. Choi, D. Couriel,

P. Reddy, J. L. M. Ferrara, S. Paczesny, ST2 as a marker for risk of therapy-resistant graft-versus-host disease and death. *N Engl J Med* **369**, 529–539 (2013).

13. M. J. Hartwell, U. Özbek, E. Holler, A. S. Renteria, H. Major-Monfried, P. Reddy, M. Aziz, W. J. Hogan, F. Ayuk, Y. A. Efebera, E. O. Hexner, U. Bunworasate, M. Qayed, R. Ordemann, M. Wölfl, S. Mielke, A. Pawarode, Y.-B. Chen, S. Devine, A. C. Harris, M. Jagasia, C. L. Kitko, M. R. Litzow, N. Kröger, F. Locatelli, G. Morales, R. Nakamura, R. Reshef, W. Rösler, D. Weber, K. Wudhikarn, G. A. Yanik, J. E. Levine, J. L. Ferrara, An early-biomarker algorithm predicts lethal graft-versus-host disease and survival. *JCI Insight* **2**, e89798 (2017).

14. H. Major-Monfried, A. S. Renteria, A. Pawarode, P. Reddy, F. Ayuk, E. Holler, Y. A. Efebera, W. J. Hogan, M. Wölfl, M. Qayed, E. O. Hexner, K. Wudhikarn, R. Ordemann, R. Young, J. Shah, M. J. Hartwell, M. S. Chaudhry, M. Aziz, A. Etra, G. A. Yanik, N. Kröger, D. Weber, Y.-B. Chen, R. Nakamura, W. Rösler, C. L. Kitko, A. C. Harris, M. Pulsipher, R. Reshef, S. Kowalyk, G. Morales, I. Torres, U. Özbek, J. L. M. Ferrara, J. E. Levine, MAGIC biomarkers predict long-term outcomes for steroid-resistant acute GVHD. *Blood* **131**, 2846–2855 (2018).

15. G. Socié, D. Niederwieser, N. von Bubnoff, M. Mohty, J. Szer, R. Or, J. Garrett, A. Prahallad, C. Wilke, R. Zeiser, Prognostic value of blood biomarkers in steroid-refractory or steroid-dependent acute graft-versus-host disease: a REACH2 analysis. *Blood* **141**, 2771–2779 (2023).

16. Q. Song, X. Wang, X. Wu, T. H. Kang, H. Qin, D. Zhao, R. R. Jenq, M. R. M. van den Brink, A. D. Riggs, P. J. Martin, Y.-Z. Chen, D. Zeng, IL-22-dependent dysbiosis and mononuclear phagocyte depletion contribute to steroid-resistant gut graft-versus-host disease in mice. *Nat Commun* **12**, 805 (2021).

17. V. Arnhold, W. Y. Chang, S. A. Jansen, G. Thangavelu, M. Calafiore, P. Vinci, Y.-Y. Fu, T. Ito, S. Takashima, A. Egorova, J. Kuttiyara, A. Perlstein, M. van Hoesel, C. Liu, B. R.

Blazar, C. A. Lindemans, A. M. Hanash, Corticosteroids impair epithelial regeneration in immune-mediated intestinal damage. *J Clin Invest* **134**, e155880 (2024).

18. T. Toubai, C. Rossi, I. Tawara, C. Liu, C. Zajac, K. Oravecz-Wilson, D. Peltier, Y. Sun, H. Fujiwara, S.-R. Wu, M. Riwes, I. Henig, S. Kim, P. Reddy, Murine Models of Steroid Refractory Graft-versus-Host Disease. *Sci Rep* **8**, 12475 (2018).

19. S. G. Holtan, A. Shabaneh, B. C. Betts, A. Rashidi, M. L. MacMillan, C. Ustun, K. Amin, B. P. Vaughn, J. Howard, A. Khoruts, M. Arora, T. E. DeFor, D. Johnson, B. R. Blazar, D. J. Weisdorf, J. Wang, Stress responses, M2 macrophages, and a distinct microbial signature in fatal intestinal acute graft-versus-host disease. *JCI Insight* **5**, e129762, 129762 (2019).

20. L. Schwab, L. Goroncy, S. Palaniyandi, S. Gautam, A. Triantafyllopoulou, A. Mocsai, W. Reichardt, F. J. Karlsson, S. V. Radhakrishnan, K. Hanke, A. Schmitt-Graeff, M. Freudenberg, F. D. von Loewenich, P. Wolf, F. Leonhardt, N. Baxan, D. Pfeifer, O. Schmah, A. Schönle, S. F. Martin, R. Mertelsmann, J. Duyster, J. Finke, M. Prinz, P. Henneke, H. Häcker, G. C. Hildebrandt, G. Häcker, R. Zeiser, Neutrophil granulocytes recruited upon translocation of intestinal bacteria enhance graft-versus-host disease via tissue damage. *Nat Med* **20**, 648–654 (2014).

21. J. Hülsdünker, K. J. Ottmüller, H. P. Neeff, M. Koyama, Z. Gao, O. S. Thomas, M. Follo, A. Al-Ahmad, G. Prinz, S. Duquesne, H. Dierbach, S. Kirschnek, T. Lämmermann, M. J. Blaser, B. T. Fife, B. R. Blazar, A. Beilhack, G. R. Hill, G. Häcker, R. Zeiser, Neutrophils provide cellular communication between ileum and mesenteric lymph nodes at graft-versus-host disease onset. *Blood* **131**, 1858–1869 (2018).

22. M. Pelletier, L. Maggi, A. Micheletti, E. Lazzeri, N. Tamassia, C. Costantini, L. Cosmi, C. Lunardi, F. Annunziato, S. Romagnani, M. A. Cassatella, Evidence for a cross-talk between human neutrophils and Th17 cells. *Blood* **115**, 335–343 (2010).

23. D. Minns, K. J. Smith, V. Alessandrini, G. Hardisty, L. Melrose, L. Jackson-Jones, A. S. MacDonald, D. J. Davidson, E. Gwyer Findlay, The neutrophil antimicrobial peptide cathelicidin promotes Th17 differentiation. *Nat Commun* **12**, 1285 (2021).

24. Q. Song, U. Nasri, D. Zeng, Steroid-Refractory Gut Graft-Versus-Host Disease: What We Have Learned From Basic Immunology and Experimental Mouse Model. *Front Immunol* **13**, 844271 (2022).

25. B. K. Patel, M. J. Raabe, E. R. Lang, Y. Song, C. Lu, V. Deshpande, L. T. Nieman, M. J. Aryee, Y.-B. Chen, D. T. Ting, Z. DeFilipp, Spatial transcriptomics reveals distinct tissue niches linked with steroid responsiveness in acute gastrointestinal GVHD. *Blood* **142**, 1831–1844 (2023).

26. R. R. Jenq, Y. Taur, S. M. Devlin, D. M. Ponce, J. D. Goldberg, K. F. Ahr, E. R. Littmann, L. Ling, A. C. Gobourne, L. C. Miller, M. D. Docampo, J. U. Peled, N. Arpaia, J. R. Cross, T. K. Peets, M. A. Lumish, Y. Shono, J. A. Dudakov, H. Poeck, A. M. Hanash, J. N. Barker, M.-A. Perales, S. A. Giralt, E. G. Pamer, M. R. M. van den Brink, Intestinal Blautia Is Associated with Reduced Death from Graft-versus-Host Disease. *Biol Blood Marrow Transplant* **21**, 1373–1383 (2015).

27. Y. Furusawa, Y. Obata, S. Fukuda, T. A. Endo, G. Nakato, D. Takahashi, Y. Nakanishi, C. Uetake, K. Kato, T. Kato, M. Takahashi, N. N. Fukuda, S. Murakami, E. Miyauchi, S. Hino, K. Atarashi, S. Onawa, Y. Fujimura, T. Lockett, J. M. Clarke, D. L. Topping, M. Tomita, S. Hori, O. Ohara, T. Morita, H. Koseki, J. Kikuchi, K. Honda, K. Hase, H. Ohno, Commensal microbe-derived butyrate induces the differentiation of colonic regulatory T cells. *Nature* **504**, 446–450 (2013).

28. N. D. Mathewson, R. Jenq, A. V. Mathew, M. Koenigsknecht, A. Hanash, T. Toubai, K. Oravecz-Wilson, S.-R. Wu, Y. Sun, C. Rossi, H. Fujiwara, J. Byun, Y. Shono, C. Lindemans, M. Calafiore, T. M. Schmidt, K. Honda, V. B. Young, S. Pennathur, M. van den Brink, P. Reddy, Gut microbiome-derived metabolites modulate intestinal epithelial cell damage and mitigate graft-versus-host disease. *Nat Immunol* **17**, 505–513 (2016).

29. J. L. Golob, M. M. DeMeules, T. Loeffelholz, Z. Z. Quinn, M. K. Dame, S. S. Silvestri, M. C. Wu, T. M. Schmidt, T. L. Fiedler, M. J. Hoostal, M. Mielcarek, J. Spence, S. A. Pergam, D. N. Fredricks, Butyrogenic bacteria after acute graft-versus-host disease (GVHD) are associated with the development of steroid-refractory GVHD. *Blood Adv* **3**, 2866–2869 (2019).

30. M. Couturier, B. Lamarthée, J. Arbez, J.-C. Renauld, C. Bossard, F. Malard, F. Bonnefoy, M. Mohty, S. Perruche, P. Tiberghien, P. Saas, B. Gaugler, IL-22 deficiency in donor T cells attenuates murine acute graft-versus-host disease mortality while sparing the graft-versus-leukemia effect. *Leukemia* **27**, 1527–1537 (2013).

31. B. Lamarthée, F. Malard, C. Gamonet, C. Bossard, M. Couturier, J.-C. Renauld, M. Mohty, P. Saas, B. Gaugler, Donor interleukin-22 and host type I interferon signaling pathway participate in intestinal graft-versus-host disease via STAT1 activation and CXCL10. *Mucosal Immunol* **9**, 309–321 (2016).

32. M. A. Schroeder, J. F. DiPersio, Mouse models of graft-versus-host disease: advances and limitations. *Disease Models & Mechanisms* **4**, 318–333 (2011).

33. R. Browaeys, W. Saelens, Y. Saeys, NicheNet: modeling intercellular communication by linking ligands to target genes. *Nat Methods* **17**, 159–162 (2020).

34. D. R. Edwards, M. M. Handsley, C. J. Pennington, The ADAM metalloproteinases. *Mol Aspects Med* **29**, 258–289 (2008).

35. J. C. Albring, M. M. Sandau, A. S. Rapaport, B. T. Edelson, A. Satpathy, M. Mashayekhi, S. K. Lathrop, C.-S. Hsieh, M. Stelljes, M. Colonna, T. L. Murphy, K. M. Murphy, Targeting of B and T lymphocyte associated (BTLA) prevents graft-versus-host disease without global immunosuppression. *J Exp Med* **207**, 2551–2559 (2010).

36. Y. Sakoda, J.-J. Park, Y. Zhao, A. Kuramasu, D. Geng, Y. Liu, E. Davila, K. Tamada, Dichotomous regulation of GVHD through bidirectional functions of the BTLA-HVEM pathway. *Blood* **117**, 2506–2514 (2011).

37. F. Martins, E. Planet, D. Marino, M. Ansari, D. Trono, Single-cell transcriptome analysis reveals atypical monocytes circulating ahead of acute graft-versus-host disease clinical onset. *J Leukoc Biol*, qiae229 (2024).

38. H. Sun, L. Wu, X. Zhao, Y. Huo, P. Dong, A. Pang, Y. Zheng, Y. Han, S. Ma, E. Jiang, F. Dong, T. Cheng, S. Hao, Monocytes as an early risk factor for acute graft-versus-host disease after allogeneic hematopoietic stem cell transplantation. *Front Immunol* **15**, 1433091 (2024).

39. L. Jardine, U. Cytlak, M. Gunawan, G. Reynolds, K. Green, X.-N. Wang, S. Pagan, M. Paramitha, C. A. Lamb, A. K. Long, E. Hurst, S. Nair, G. H. Jackson, A. Publicover, V. Bigley, M. Haniffa, A. J. Simpson, M. Collin, Donor monocyte-derived macrophages promote human acute graft-versus-host disease. *J Clin Invest* **130**, 4574–4586 (2020).

40. K. Seno, M. Yasunaga, H. Kajiya, K. Izaki-Hagio, H. Morita, M. Yoneda, T. Hirofuji, J. Ohno, Dynamics of M1 macrophages in oral mucosal lesions during the development of acute graft-versus-host disease in rats. *Clin Exp Immunol* **190**, 315–327 (2017).

41. J. E. Levine, S. Paczesny, S. Mineishi, T. Braun, S. W. Choi, R. J. Hutchinson, D. Jones, Y. Khaled, C. L. Kitko, D. Bickley, O. Krijanovski, P. Reddy, G. Yanik, J. L. M. Ferrara, Etanercept plus methylprednisolone as initial therapy for acute graft-versus-host disease. *Blood* **111**, 2470–2475 (2008).

42. R. J. Robb, G. R. Hill, The interferon-dependent orchestration of innate and adaptive immunity after transplantation. *Blood* **119**, 5351–5358 (2012).

43. S. Wang, T. Cheng, X. Chen, C. Zeng, W. Qin, Y. Xu, IFN-γ induces acute graft-versus-host disease by promoting HMGB1-mediated nuclear-to-cytoplasm translocation and autophagic degradation of p53. *Clin Sci (Lond)* **138**, 1287–1304 (2024).

44. H. Okamura, H. Tsutsi, T. Komatsu, M. Yutsudo, A. Hakura, T. Tanimoto, K. Torigoe, T. Okura, Y. Nukada, K. Hattori, Cloning of a new cytokine that induces IFN-gamma production by T cells. *Nature* **378**, 88–91 (1995).

45. Y. Fujimori, H. Takatsuka, Y. Takemoto, H. Hara, H. Okamura, K. Nakanishi, E. Kakishita, Elevated interleukin (IL)-18 levels during acute graft-versus-host disease after allogeneic bone marrow transplantation. *Br J Haematol* **109**, 652–657 (2000).

46. S. W. Choi, G. C. Hildebrandt, K. M. Olkiewicz, D. A. Hanauer, M. N. Chaudhary, I. A. Silva, C. E. Rogers, D. T. Deurloo, J. M. Fisher, C. Liu, D. Adams, S. W. Chensue, K. R. Cooke, CCR1/CCL5 (RANTES) receptor-ligand interactions modulate allogeneic T-cell responses and graft-versus-host disease following stem-cell transplantation. *Blood* **110**, 3447–3455 (2007).

47. S. DeWolf, Y. Elhanati, K. Nichols, N. R. Waters, C. L. Nguyen, J. B. Slingerland, N. Rodriguez, O. Lyudovyk, P. A. Giardina, A. I. Kousa, H. Andrlová, N. Ceglia, T. Fei, R. Kappagantula, Y. Li, N. Aleynick, P. Baez, R. Murali, A. Hayashi, N. Lee, B. Gipson, M. Rangesa, Z. Katsamakis, A. Dai, A. G. Blouin, M. Arcila, I. Masilionis, R. Chaligne, D. M. Ponce, H. J. Landau, I. Politikos, R. Tamari, A. M. Hanash, R. R. Jenq, S. A. Giralt, K. A. Markey, Y. Zhang, M.-A. Perales, N. D. Socci, B. D. Greenbaum, C. A. Iacobuzio-Donahue, T. J. Hollmann, M. R. M. van den Brink, J. U. Peled, Tissue-specific features of the T cell repertoire after allogeneic hematopoietic cell transplantation in human and mouse. *Sci Transl Med* **15**, eabq0476 (2023).

48. S. D. Schutt, Y. Wu, A. Kharel, D. Bastian, H.-J. Choi, M. Hanief Sofi, C. Mealer, B. McDaniel Mims, H. Nguyen, C. Liu, K. Helke, W. Cui, X. Zhang, Y. Ben-David, X.-Z. Yu, The druggable transcription factor Fli-1 regulates T cell immunity and tolerance in graft-versus-host disease. *J Clin Invest* **132**, e143950 (2022).

49. Y. Hao, S. Hao, E. Andersen-Nissen, W. M. Mauck, S. Zheng, A. Butler, M. J. Lee, A. J. Wilk, C. Darby, M. Zager, P. Hoffman, M. Stoeckius, E. Papalexi, E. P. Mimitou, J. Jain, A. Srivastava, T. Stuart, L. M. Fleming, B. Yeung, A. J. Rogers, J. M. McElrath, C. A. Blish, R. Gottardo, P. Smibert, R. Satija, Integrated analysis of multimodal single-cell data. *Cell* **184**, 3573-3587.e29 (2021).

50. G. Korotkevich, V. Sukhov, N. Budin, B. Shpak, M. N. Artyomov, A. Sergushichev, Fast gene set enrichment analysis. bioRxiv [Preprint] (2021). https://doi.org/10.1101/060012.

51. A. Liberzon, C. Birger, H. Thorvaldsdóttir, M. Ghandi, J. P. Mesirov, P. Tamayo, The Molecular Signatures Database (MSigDB) hallmark gene set collection. *Cell Syst* **1**, 417–425 (2015).

52. J. A. Ramilowski, T. Goldberg, J. Harshbarger, E. Kloppmann, M. Lizio, V. P. Satagopam, M. Itoh, H. Kawaji, P. Carninci, B. Rost, A. R. R. Forrest, A draft network of ligand-receptor-mediated multicellular signalling in human. *Nat Commun* **6**, 7866 (2015).

53. A. J. Pawson, J. L. Sharman, H. E. Benson, E. Faccenda, S. P. H. Alexander, O. P. Buneman, A. P. Davenport, J. C. McGrath, J. A. Peters, C. Southan, M. Spedding, W. Yu, A. J. Harmar, NC-IUPHAR, The IUPHAR/BPS Guide to PHARMACOLOGY: an expert-driven knowledgebase of drug targets and their ligands. *Nucleic Acids Res* **42**, D1098-1106 (2014).

54. A. D. Rouillard, G. W. Gundersen, N. F. Fernandez, Z. Wang, C. D. Monteiro, M. G. McDermott, A. Ma'ayan, The harmonizome: a collection of processed datasets gathered to serve and mine knowledge about genes and proteins. *Database (Oxford)* **2016**, baw100 (2016).

55. K. Street, D. Risso, R. B. Fletcher, D. Das, J. Ngai, N. Yosef, E. Purdom, S. Dudoit, Slingshot: cell lineage and pseudotime inference for single-cell transcriptomics. *BMC Genomics* **19**, 477 (2018).

56. K. Van den Berge, H. Roux de Bézieux, K. Street, W. Saelens, R. Cannoodt, Y. Saeys, S. Dudoit, L. Clement, Trajectory-based differential expression analysis for single-cell sequencing data. *Nat Commun* **11**, 1201 (2020).

57. G. Yu, L.-G. Wang, Y. Han, Q.-Y. He, clusterProfiler: an R package for comparing biological themes among gene clusters. *OMICS* **16**, 284–287 (2012).

58. M. Ashburner, C. A. Ball, J. A. Blake, D. Botstein, H. Butler, J. M. Cherry, A. P. Davis, K. Dolinski, S. S. Dwight, J. T. Eppig, M. A. Harris, D. P. Hill, L. Issel-Tarver, A. Kasarskis,

S. Lewis, J. C. Matese, J. E. Richardson, M. Ringwald, G. M. Rubin, G. Sherlock, Gene Ontology: tool for the unification of biology. *Nat Genet* **25**, 25–29 (2000).

59. The Gene Ontology Consortium, S. A. Aleksander, J. Balhoff, S. Carbon, J. M. Cherry, H. J. Drabkin, D. Ebert, M. Feuermann, P. Gaudet, N. L. Harris, D. P. Hill, R. Lee, H. Mi, S. Moxon, C. J. Mungall, A. Muruganugan, T. Mushayahama, P. W. Sternberg, P. D. Thomas, K. Van Auken, J. Ramsey, D. A. Siegele, R. L. Chisholm, P. Fey, M. C. Aspromonte, M. V. Nugnes, F. Quaglia, S. Tosatto, M. Giglio, S. Nadendla, G. Antonazzo, H. Attrill, G. dos Santos, S. Marygold, V. Strelets, C. J. Tabone, J. Thurmond, P. Zhou, S. H. Ahmed, P. Asanitthong, D. Luna Buitrago, M. N. Erdol, M. C. Gage, M. Ali Kadhum, K. Y. C. Li, M. Long, A. Michalak, A. Pesala, A. Pritazahra, S. C. C. Saverimuttu, R. Su, K. E. Thurlow, R. C. Lovering, C. Logie, S. Oliferenko, J. Blake, K. Christie, L. Corbani, M. E. Dolan, H. J. Drabkin, D. P. Hill, L. Ni, D. Sitnikov, C. Smith, A. Cuzick, J. Seager, L. Cooper, J. Elser, P. Jaiswal, P. Gupta, P. Jaiswal, S. Naithani, M. Lera-Ramirez, K. Rutherford, V. Wood, J. L. De Pons, M. R. Dwinell, G. T. Hayman, M. L. Kaldunski, A. E. Kwitek, S. J. F. Laulederkind, M. A. Tutaj, M. Vedi, S.-J. Wang, P. D'Eustachio, L. Aimo, K. Axelsen, A. Bridge, N. Hyka-Nouspikel, A. Morgat, S. A. Aleksander, J. M. Cherry, S. R. Engel, K. Karra, S. R. Miyasato, R. S. Nash, M. S. Skrzypek, S. Weng, E. D. Wong, E. Bakker, T. Z. Berardini, L. Reiser, A. Auchincloss, K. Axelsen, G. Argoud-Puy, M.-C. Blatter, E. Boutet, L. Breuza, A. Bridge, C. Casals-Casas, E. Coudert, A. Estreicher, M. Livia Famiglietti, M. Feuermann, A. Gos, N. Gruaz-Gumowski, C. Hulo, N. Hyka-Nouspikel, F. Jungo, P. Le Mercier, D. Lieberherr, P. Masson, A. Morgat, I. Pedruzzi, L. Pourcel, S. Poux, C. Rivoire, S. Sundaram, A. Bateman, E. Bowler-Barnett, H. Bye-A-Jee, P. Denny, A. Ignatchenko, R. Ishtiaq, A. Lock, Y. Lussi, M. Magrane, M. J. Martin, S. Orchard, P. Raposo, E. Speretta, N. Tyagi, K. Warner, R. Zaru, A. D. Diehl, R. Lee, J. Chan, S. Diamantakis, D. Raciti, M. Zarowiecki, M. Fisher, C. James-Zorn, V. Ponferrada, A. Zorn, S. Ramachandran, L. Ruzicka, M. Westerfield, The Gene Ontology knowledgebase in 2023. *Genetics* **224**, iyad031 (2023).

Acknowledgments:

The authors thank the patients who agreed to participate in this study by providing their blood samples. We also thank the iGenSeq platform at ICM for sequencing the PBMC samples. We are grateful to the CRYOSTEM biobank for collecting patient samples and clinical data.

Funding:

This project was funded by la Fédération Leucémie Espoir and Fondation Maladies Rare (HPN-AM).

Author contributions:

Conceptualization: SLG, DM

Methodology: SLG, NV, DM

Samples processing: SLG, DB, YM, EB

Investigation: SLG, NV, DM

Visualization: SLG, GS, RPD, NV, DM

Funding acquisition: DM

Project administration: EB, DM, GS, RPD

Supervision: NV, DM

Writing – original draft: SLG, NV, DM

Draft revision: SLG, YM, DB, EB, RPF, GS, NV, DM

Competing interests:

Authors declare that they have no competing interests.

Data availability

Raw data are available on GEO public repository: GSE229733. A private reviewer access has been provided with the following secured token: ynmbkwaknfebdwb

Source code to reproduce the analyses, figures, and tables described in this manuscript are provided in a Git repository: https://gitlab.com/SophieLG/gvh_transcriptomic and long term preserved in Software Heritage:

https://archive.softwareheritage.org/browse/origin/directory/?origin_url=https://gitlab.com/SophieLG/gvh_transcriptomic&timestamp=2024-12-09T14:03:56.753000%2B00:00

Figures legends:

Figure 1: Patients and cells characterization.

A: Experimental design: HSCT patients (n=53) with (n=21) and without aGVHD (n=32) and healthy donor as control group (n=6) were analyzed. PBMC were collected at day 100 post HSCT for patients without aGVHD, and before steroid initiation for patients with aGVHD. **B:** Number of cells included in the analysis after CITE-Seq processing. **C:** Uniform Manifold Approximation and Projection (UMAP) after principal component analysis for immune cells clusterisation, according to surface markers. **D:** Heatmap depicting immune cluster's identification through surface antigen expression. Three irrelevant populations were removed and are shown in **Figure S1**. **E**: Volcano plot exhibiting immune cells abundance in GVHD or non-GVHD condition. Y axis reflects que -log 10(adjusted p-value) from differential expression output, using non-parametric Mann-Whitney-Wilcoxon rank sum test. X axis reflects the log(ratio) of median abundance in aGVHD condition, over non-aGVHD condition. Abbreviation: CITE-Seq: Cellular indexing of transcriptomes and epitopes sequencing. aGVHD: acute graft versus host disease. HSCT: allogeneic hematopoietic stem cell transplantation. PBMC: Peripheral Blood Mononuclear Cells. SS-aGVHD: steroid sensitive acute graft versus host disease. SR-aGVHD: steroid resistant acute graft versus host disease.

Figure 2: Immunotypes distinguished different immune patterns associated with aGVHD incidence.

A: Principal coordinates analysis (PCoA) revealed 4 different immune clusters (immunotypes) according to cell population composition. **B:** Distribution of aGVHD patients among immunotypes (left panel) and corticosteroid sensitivity (right panel). Fisher test was used for statistical analysis. **C:** GVHD cumulative incidence with death as competing risk, estimated by Kaplan-Meir method, Logrank test was used for statistical analysis. Immunotype 4 cumulative incidence at day 100 = 72%, Immunotype 3 cumulative incidence at day 100 = 0%, Immunotype 2 cumulative incidence at day 100 = 38%, Immunotype 1 cumulative incidence at

day 100 = 55%, log-rank p-value = 0.005. **D:** Bar plots showing top 15 contributing immune subsets to immunotypes. Contribution was determined with permutational multivariate analysis of variance (PERMANOVA).

Figure 3: Cell cycle scoring and enrichment pathways

A: Volcano plots exhibiting cell cycle analysis after cell cycle phases scoring. X axis represents log ratio of median number of cells in each phase in aGVHD patients over non GVHD patients. Y axis represents log adjusted p values. Immune population significantly increased or decreased are marked in red. Mann-Whitney-Wilcoxon tests were performed for statistical analysis, and p values were adjusted using Benjamini and Hochberg method. **B:** Pathways enrichment analysis comparing SR and SS-aGVHD, using gene set enrichment method and "hallmarks" gene reference data set. Only significant values with adjusted p-value < 0.05 are shown. NES: normalized enrichment score. SS-aGVHD: steroid sensitive acute graft versus host disease. SR-aGVHD: steroid resistant acute graft versus host disease.

Figure 4: Cell-cell interactions with CD8+ T cells as receiver revealed specific patterns associated with SR-aGVHD

NicheNet Output when focusing on CD8+ T cells as receiver is depicted on panel A, B and C. **A:** Expression of top-ranked ligands on sender cells. Prioritized ligands identified are exhibited on Y axis, and sender cells on X axis. The color determines the average expression and the point size the percent of senders expressing the ligand. **B:** Relative expression of ligands on sender cells. Expression is exhibited in log fold change (red: increase expression in SR-aGVHD patients, Blue: decreased expression in SR-aGVHD patients). **C:** Ligand–target matrix exhibiting the regulatory potential of interactions. On the X axis is shown the active targets genes of the top-ranked ligands. Heatmap visualization showing which top-ranked ligands are predicted to have regulated the expression of which differentially expressed genes. **D:** Circos plots depicting interactions between senders and all receiver cells. Ligands are

shown on the left side of the circos plot, and targets on the right side. Only *bona fide* interactions were selected (**Figure S8**). Links exhibits positive log fold change (left panel, increased in SR-aGVHD patients) or negative log fold change (right panel, increased in SS-aGVHD patients) from “ligand differential expression heatmap” NicheNet’s output. The thickness of the link represents the numbers of sender populations involved in the interaction. SR-aGVHD: Steroid resistant acute graft versus host disease. SS-aGVHD: Steroid sensitive acute graft versus host disease.

Figure 5: SR-aGVHD is associated with specific trajectory in CD8$^+$ T cells

A: Density plot for number of cells according to lineage 1 pseudotime visualization. SR-aGVHD cell abundance was marked in low and high pseudotimes, while SS-aGVHD was associated with a continuous increase in cell abundance along differentiation. **B:** Lineage 1 trajectory on RNA clusterization. **C:** Heatmap depicting gene expression among the top 500 most expressed genes in SS-aGVHD patient (top panel) and in SR-aGVHD patients (low panel), along pseudotime. The color at the top of each heatmap represents the immune population in which the gene is expressed. **D:** Expression along pseudotime of four of the top 100 genes, whose expression varied the most between the start and end points of a lineage. **E:** Over-representation analysis to identify pathways associated with genes expression from each module of the heatmaps. Only pathways associated with adjusted pval < 0.05 from “molecular functions” and “biological process” of the Gene Ontology knowledgbase(*58*, *59*) were selected for dot plots visualisation. SR-aGVHD: Steroid resistant acute graft versus host disease. SS-aGVHD: Steroid sensitive acute graft versus host disease.

Fig. S1: Immune populations in each group of patients:

HSCT: hematopoietic Stem Cell Transplantation. GVHD: Graft Vetsus Host Disease.

Fig. S2: Immunotype survival analysis:

Survival analyses according to immunotypes

Fig. S3: Immunotype and clinical variables:

Clinical parameters and immunotypes.

Fig. S4: Immune cell abundance in SS- and SR-GVHD patients:

Volcano plot exhibiting immune cells abundance in SR-GVHD and SS-GVHD condition. Y axis reflects que -log 10(adjusted p-value) from differential expression output, using non-parametric Wilcoxon rank sum test. X axis reflects the log(ratio) of median abundance in SR-GVHD condition, over SS-GVHD condition. Abbreviation: GVHD: graft versus host disease. HSCT: allogeneic hematopoietic stem cell transplantation. SS-GVHD: Steroid Sensitive acute graft versus host disease. SR-GVHD: Steroid resistant acute graft versus host disease.

Fig. S5: Cell cycle in SS- and SR-GVHD patients and enrichment pathways in aGVHD:

Volcano plots exhibiting cell cycle analysis after cell cycle phases scoring. X axis represents log ratio of median number of cells in each phase in SR-GVHD patients over SS-GVHD patients. Y axis represents log adjusted p values. Immune population significantly increased or decreased are marked in red. Mann-Whitney-Wilcoxon tests were performed for statistical analysis, and p values were adjusted using Benjamini and Hochberg method.

Fig. S6: Pathway enrichments in aGVHD patients:

Pathways enrichment analysis comparing aGVHD and no GVHD, using gene set enrichment method and “hallmarks” gene reference data set. Only significant values with adjusted

p-value < 0.05 are shown. NES: normalized enrichment score. SS-GVHD: Steroid Sensitive acute graft versus host disease. SR-GVHD: Steroid resistant acute graft versus host disease.

Fig. S7: Interactions combined plots in regulatory T cells and NK cells:

A: Combined plots of cell-cell interactions analysis, with T regulators lymphocytes as receiver. **B:** Combined plots of cell-cell interactions analysis, with NK cells as receiver.

Fig. S8: Interactions combined plots in $CD4^+$ T cells and double negative T cells

A: Combined plots of cell-cell interactions analysis, with $CD4^+$ T lymphocytes as receiver. **B:** Combined plots of cell-cell interactions analysis, with double negative T cells as receiver.

Fig. S9: Bona fide interactions in all receivers:

A: Known interactions (*bona fide*) with prioritized ligands of each receiver populations. **B:** Increased and decreased interactions in patients with aGVHD, according to *bona fide* interactions.

Fig. S10: Clustering based on RNA expression

A: Clusters based on mRNA expression. Immune cells were identified using protein surface expression after clustering. **B:** Immune cells on UMAP in GVHD patients, no GVHD patients and healthy donors.

Fig. S11: $CD8^+$ T cells lineage 2 trajectory analysis:

A: Density plot for number of cells according to lineage 2 pseudotime visualization. SR-GVHD cell abundance was marked in low and high pseudotimes, while SS-GVHD was associated with a continuous increase in cell abundance along differentiation. **B:** Lineage 2 trajectory on RNA clusterisation. **C:** Heatmap of RNA expression of the 500 most expressed gene in SS-GVHD patient (top panel) and in SR-GVHD patients (low panel), along pseudotime. The

color at the top of each heatmap represents the immune population in which the gene is expressed. **D:** Expression along pseudotime of four of the top 100 genes, whose expression varied the most between the start and end points of a lineage. **E:** Over-representation analysis to identify pathways associated with genes expression from each module of the heatmaps. Only pathways associated with adjusted pval < 0.05 from “molecular functions” and “biological process” of the Gene Ontology knowledgbase(*58*, *59*) were selected for dot plots visualisation. SR–GVHD: Steroid resistant graft versus host disease. SS–GVHD: Steroid sensitive graft versus host disease.

Fig. S12: Over representation analysis in lineage 1 SR-GVHD patients:
Over-representation analysis in lineage 1 and SR-GVHD patients to identify pathways associated with genes expression from each module of the heatmaps. Only pathways associated with adjusted pval < 0.05 from “molecular functions” and “biological process” of the Gene Ontology knowledgbase(*58*, *59*) were selected for dot plots visualisation. SR–GVHD: Steroid resistant graft versus host disease. SS–GVHD: Steroid sensitive graft versus host disease.

Fig. S13: Over representation analysis in lineage 1 SS-GVHD patients:
Over-representation analysis in lineage 1 and SS-GVHD patients to identify pathways associated with genes expression from each module of the heatmaps. Only pathways associated with adjusted pval < 0.05 from “molecular functions” and “biological process” of the Gene Ontology knowledgbase(*58*, *59*) were selected for dot plots visualisation. SR–GVHD: Steroid resistant graft versus host disease. SS–GVHD: Steroid sensitive graft versus host disease.

Fig. S14: Over representation analysis in lineage 2 SR-GVHD patients:

Over-representation analysis in lineage 2 and SR-GVHD patients to identify pathways associated with genes expression from each module of the heatmaps. Only pathways associated with adjusted pval < 0.05 from “molecular functions” and “biological process” of the Gene Ontology knowledgbase(*58*, *59*) were selected for dot plots visualisation. SR–GVHD: Steroid resistant graft versus host disease. SS–GVHD: Steroid sensitive graft versus host disease.

Fig. S15: Over representation analysis in lineage 2 SS-GVHD patients:

Over-representation analysis in lineage 2 and SS-GVHD patients to identify pathways associated with genes expression from each module of the heatmaps. Only pathways associated with adjusted pval < 0.05 from “molecular functions” and “biological process” of the Gene Ontology knowledgbase(*58*, *59*) were selected for dot plots visualisation. SR–GVHD: Steroid resistant graft versus host disease. SS–GVHD: Steroid sensitive graft versus host disease.

Table S1: Patients’ characteristics

[1]Wilcoxon rank sum exact test; Pearson's Chi-squared test; Fisher's exact test; Wilcoxon rank sum test

ALL: Acute Lymphoblastic leukemia, AML: Acute Myeloblastic Leukemia, CML: Chronic Myeloid Leukemia, CR: Complete Remission, CMV: Cytomegalovirus, GVHD: graft versus host disease, HSCT : Hematopoietic Stem Cell Transplantation, MDS: Myedlodysplastic syndrome, NA: Not applicable, NHL: Non Hodgkin Lymphoma

Table S2: Characteristics according to immunotypes:

[1]n (%); Median(Range)

[2]Fisher's exact test; Kruskal-Wallis rank sum test

ALL: Acute Lymphoblastic leukemia, AML: Acute Myeloblastic Leukemia, CML: Chronic Myeloid Leukemia, CR: Complete Remission, CMV: Cytomegalovirus, GVHD: graft versus host disease, HSCT : Hematopoietic Stem Cell Transplantation, MDS: Myedlodysplastic syndrome, NA: Not applicable, NHL: Non Hodgkin Lymphoma

Table S3: Top 500 genes expression matrix in lineage 1 SR-GVHD patients

Table S4: Top 500 genes expression matrix in lineage 1 SS-GVHD patients

Table S5: Top 500 genes expression matrix in lineage 2 SR-GVHD patients

Table S6: Top 500 genes expression matrix in lineage 2 SS-GVHD patients

Table S7: Immune population mostly represented along pseudotimes in lineage 1 SR-GVHD patients

Table S8: Immune population mostly represented along pseudotimes in lineage 1 SS-GVHD patients

Table S9: Immune population mostly represented along pseudotimes in lineage 1 2 SR-GVHD patients

Table S10: Immune population mostly represented along pseudotimes in lineage 2 SS-GVHD patients

Table S11: StartvsEnd output in lineage 1

Table S12: StartvsEnd output in lineage 2

Table S13: Total-Seq-B antibody panel

Figure 1

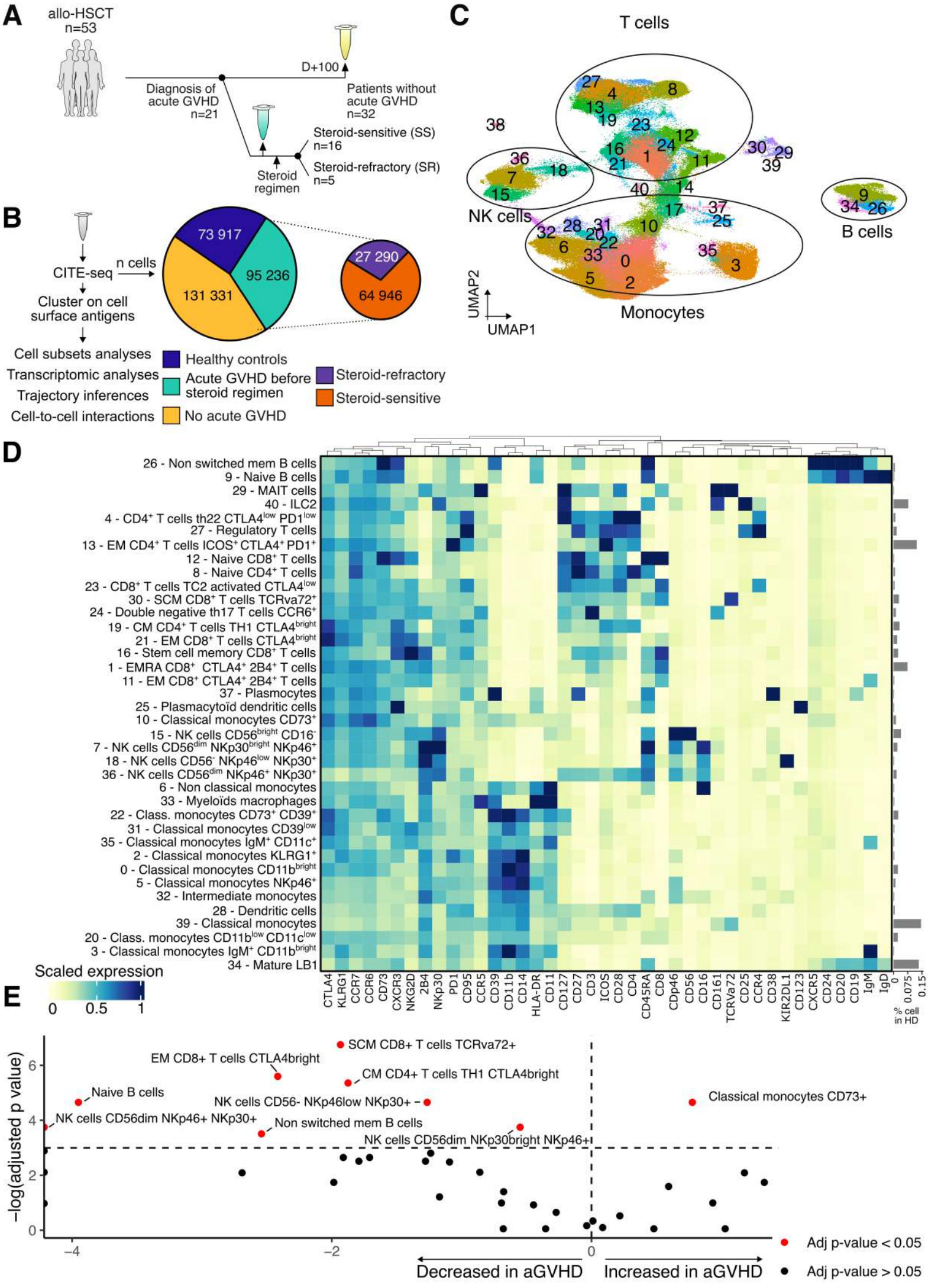
A
allo-HSCT
n=53
D+100
Diagnosis of acute GVHD n=21
Patients without acute GVHD n=32
Steroid-sensitive (SS) n=16
Steroid-refractory (SR) n=5
Steroid regimen
B
CITE-seq
n cells
Cluster on cell surface antigens
Cell subsets analyses
Transcriptomic analyses
Trajectory inferences
Cell-to-cell interactions
73 917
95 236
131 331
27 290
64 946
Healthy controls
Acute GVHD before steroid regimen
No acute GVHD
Steroid-refractory
Steroid-sensitive
C
T cells
NK cells
B cells
Monocytes
UMAP2
UMAP1
D
26 - Non switched mem B cells
9 - Naive B cells
29 - MAIT cells
40 - ILC2
4 - CD4+ T cells th22 CTLA4low PD1low
27 - Regulatory T cells
13 - EM CD4+ T cells ICOS+ CTLA4+ PD1+
12 - Naive CD8+ T cells
8 - Naive CD4+ T cells
23 - CD8+ T cells TC2 activated CTLA4low
30 - SCM CD8+ T cells TCRva72+
24 - Double negative th17 T cells CCR6+
19 - CM CD4+ T cells TH1 CTLA4bright
21 - EM CD8+ T cells CTLA4bright
16 - Stem cell memory CD8+ T cells
1 - EMRA CD8+ CTLA4+ 2B4+ T cells
11 - EM CD8+ CTLA4+ 2B4+ T cells
37 - Plasmocytes
25 - Plasmacytoïd dendritic cells
10 - Classical monocytes CD73+
15 - NK cells CD56bright CD16-
7 - NK cells CD56dim NKp30bright NKp46+
18 - NK cells CD56- NKp46low NKp30+
36 - NK cells CD56dim NKp46+ NKp30+
6 - Non classical monocytes
33 - Myeloïds macrophages
22 - Class. monocytes CD73+ CD39+
31 - Classical monocytes CD39low
35 - Classical monocytes IgM+ CD11c+
2 - Classical monocytes KLRG1+
0 - Classical monocytes CD11bbright
5 - Classical monocytes NKp46+
32 - Intermediate monocytes
28 - Dendritic cells
39 - Classical monocytes
20 - Class. monocytes CD11blow CD11clow
3 - Classical monocytes IgM+ CD11bbright
34 - Mature LB1
CTLA4 KLRG1 CCR7 CCR6 CD73 CXCR3 NKG2D 2B4 NKp30 PD1 CD95 CCR5 CD39 CD11b CD14 HLA-DR CD11 CD127 CD27 CD3 ICOS CD28 CD4 CD45RA CD8 CDp46 CD56 CD16 CD161 TCRVa72 CD25 CCR4 CD38 KIR2DL1 CD123 CXCR5 CD24 CD20 CD19 IgM IgD
% cell in HD
Scaled expression
0 0.5 1
E
SCM CD8+ T cells TCRva72+
EM CD8+ T cells CTLA4bright
CM CD4+ T cells TH1 CTLA4bright
Naive B cells
NK cells CD56- NKp46low NKp30+ -
Classical monocytes CD73+
NK cells CD56dim NKp46+ NKp30+
Non switched mem B cells
NK cells CD56dim NKp30bright NKp46+
−log(adjusted p value)
Decreased in aGVHD
Increased in aGVHD
Adj p-value < 0.05
Adj p-value > 0.05

Figure 2

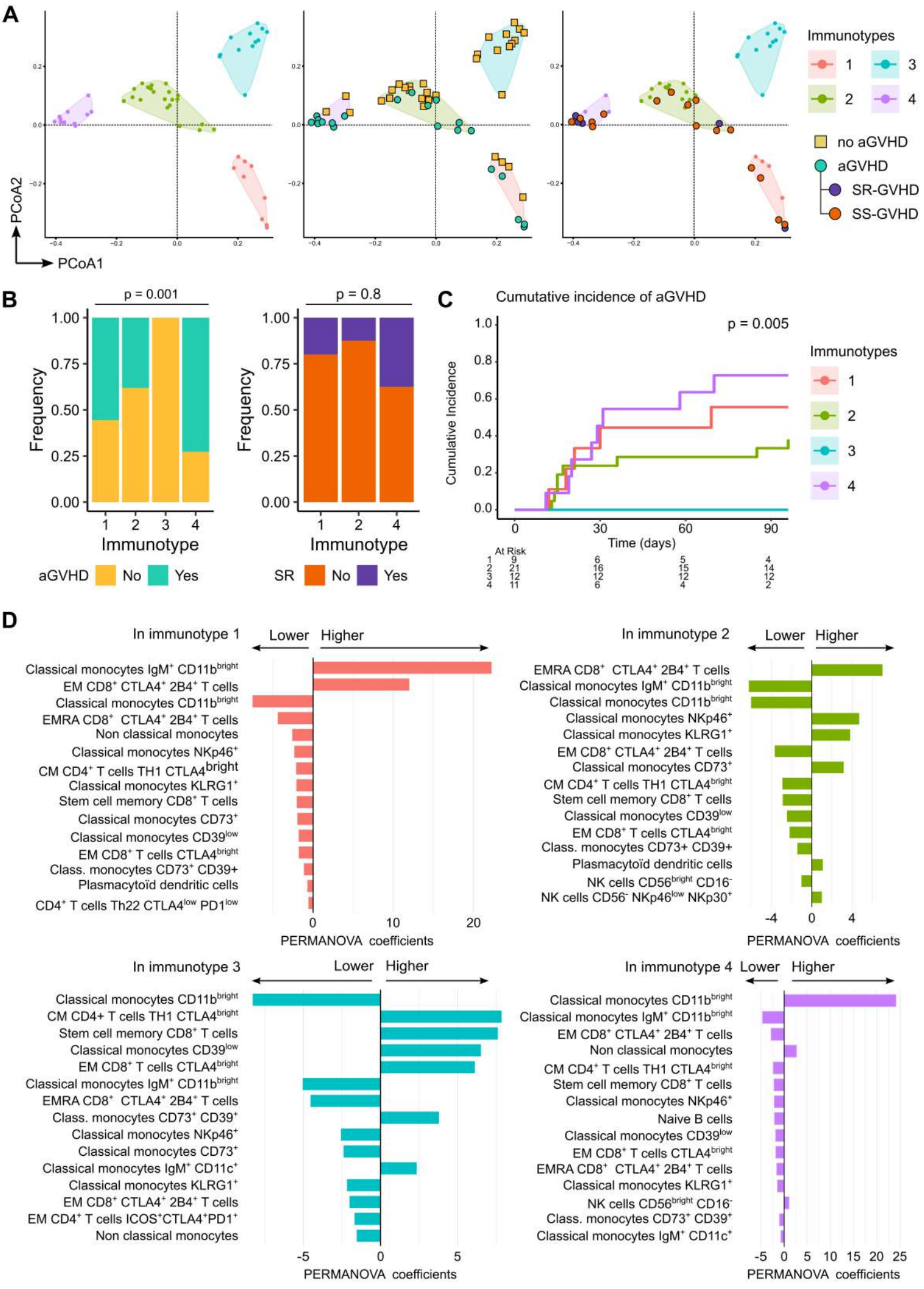
A
PCoA2
PCoA1
Immunotypes
1
2
3
4
no aGVHD
aGVHD
SR-GVHD
SS-GVHD
B
p = 0.001
p = 0.8
Frequency
Immunotype
aGVHD No Yes
SR No Yes
C
Cumutative incidence of aGVHD
p = 0.005
Cumulative Incidence
Time (days)
At Risk
D
In immunotype 1
Lower Higher
Classical monocytes IgM+ CD11b bright
EM CD8+ CTLA4+ 2B4+ T cells
Classical monocytes CD11b bright
EMRA CD8+ CTLA4+ 2B4+ T cells
Non classical monocytes
Classical monocytes NKp46+
CM CD4+ T cells TH1 CTLA4 bright
Classical monocytes KLRG1+
Stem cell memory CD8+ T cells
Classical monocytes CD73+
Classical monocytes CD39 low
EM CD8+ T cells CTLA4 bright
Class. monocytes CD73+ CD39+
Plasmacytoïd dendritic cells
CD4+ T cells Th22 CTLA4 low PD1 low
PERMANOVA coefficients
In immunotype 2
EMRA CD8+ CTLA4+ 2B4+ T cells
Classical monocytes IgM+ CD11b bright
Classical monocytes CD11b bright
Classical monocytes NKp46+
Classical monocytes KLRG1+
EM CD8+ CTLA4+ 2B4+ T cells
Classical monocytes CD73+
CM CD4+ T cells TH1 CTLA4 bright
Stem cell memory CD8+ T cells
Classical monocytes CD39 low
EM CD8+ T cells CTLA4 bright
Class. monocytes CD73+ CD39+
Plasmacytoïd dendritic cells
NK cells CD56 bright CD16-
NK cells CD56- NKp46 low NKp30+
PERMANOVA coefficients
In immunotype 3
Classical monocytes CD11b bright
CM CD4+ T cells TH1 CTLA4 bright
Stem cell memory CD8+ T cells
Classical monocytes CD39 low
EM CD8+ T cells CTLA4 bright
Classical monocytes IgM+ CD11b bright
EMRA CD8+ CTLA4+ 2B4+ T cells
Class. monocytes CD73+ CD39+
Classical monocytes NKp46+
Classical monocytes CD73+
Classical monocytes IgM+ CD11c+
Classical monocytes KLRG1+
EM CD8+ CTLA4+ 2B4+ T cells
EM CD4+ T cells ICOS+CTLA4+PD1+
Non classical monocytes
PERMANOVA coefficients
In immunotype 4
Classical monocytes CD11b bright
Classical monocytes IgM+ CD11b bright
EM CD8+ CTLA4+ 2B4+ T cells
Non classical monocytes
CM CD4+ T cells TH1 CTLA4 bright
Stem cell memory CD8+ T cells
Classical monocytes NKp46+
Naive B cells
Classical monocytes CD39 low
EM CD8+ T cells CTLA4 bright
EMRA CD8+ CTLA4+ 2B4+ T cells
Classical monocytes KLRG1+
NK cells CD56 bright CD16-
Class. monocytes CD73+ CD39+
Classical monocytes IgM+ CD11c+
PERMANOVA coefficients

Figure 3

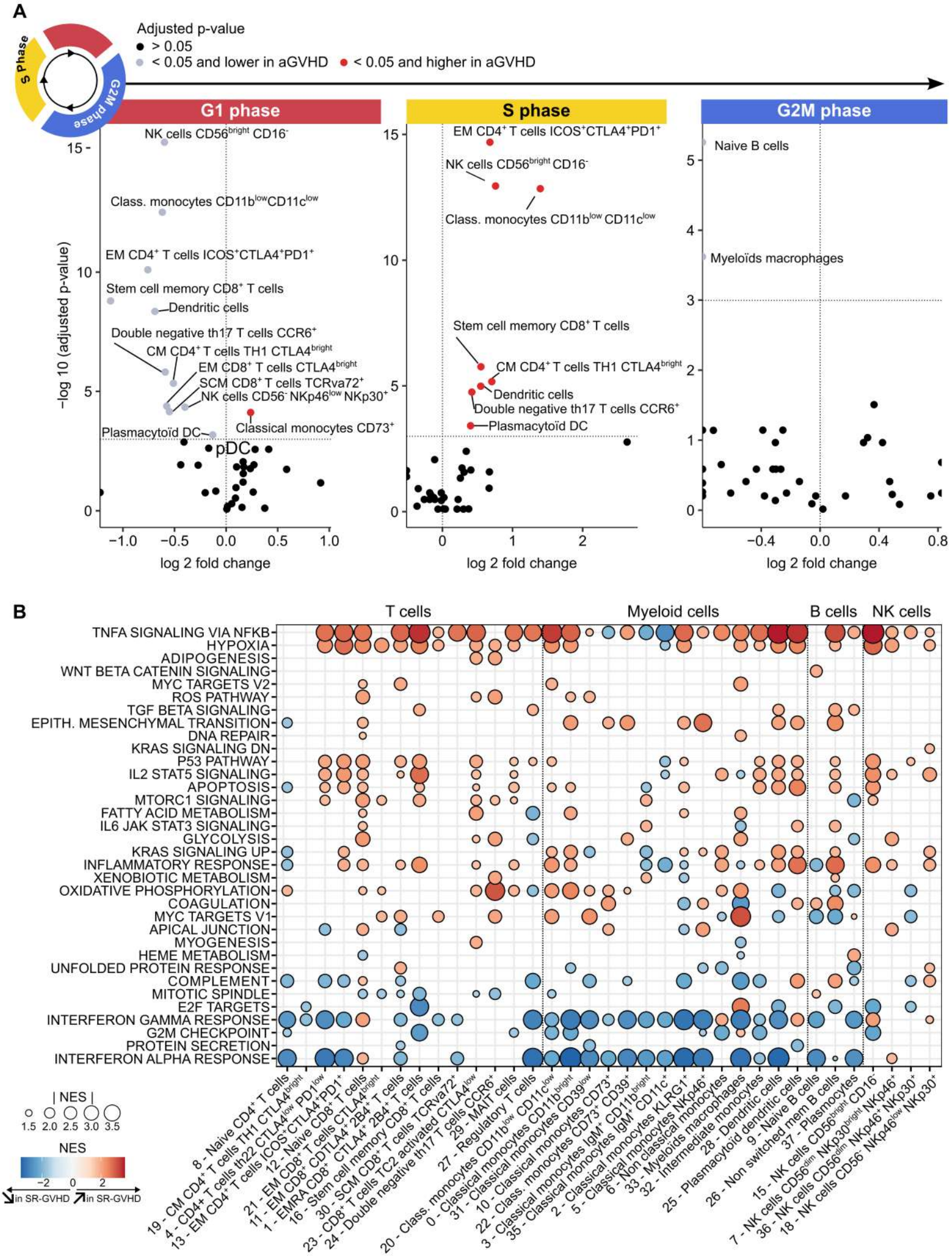
A
S Phase
G2M phase
Adjusted p-value
> 0.05
< 0.05 and lower in aGVHD
< 0.05 and higher in aGVHD
G1 phase
S phase
G2M phase
NK cells CD56bright CD16-
Class. monocytes CD11blowCD11clow
EM CD4+ T cells ICOS+CTLA4+PD1+
Stem cell memory CD8+ T cells
Dendritic cells
Double negative th17 T cells CCR6+
CM CD4+ T cells TH1 CTLA4bright
EM CD8+ T cells CTLA4bright
SCM CD8+ T cells TCRva72+
NK cells CD56- NKp46low NKp30+
Classical monocytes CD73+
Plasmacytoïd DC
pDC
Naive B cells
Myeloïds macrophages
−log 10 (adjusted p-value)
log 2 fold change
B
T cells
Myeloid cells
B cells
NK cells
TNFA SIGNALING VIA NFKB
HYPOXIA
ADIPOGENESIS
WNT BETA CATENIN SIGNALING
MYC TARGETS V2
ROS PATHWAY
TGF BETA SIGNALING
EPITH. MESENCHYMAL TRANSITION
DNA REPAIR
KRAS SIGNALING DN
P53 PATHWAY
IL2 STAT5 SIGNALING
APOPTOSIS
MTORC1 SIGNALING
FATTY ACID METABOLISM
IL6 JAK STAT3 SIGNALING
GLYCOLYSIS
KRAS SIGNALING UP
INFLAMMATORY RESPONSE
XENOBIOTIC METABOLISM
OXIDATIVE PHOSPHORYLATION
COAGULATION
MYC TARGETS V1
APICAL JUNCTION
MYOGENESIS
HEME METABOLISM
UNFOLDED PROTEIN RESPONSE
COMPLEMENT
MITOTIC SPINDLE
E2F TARGETS
INTERFERON GAMMA RESPONSE
G2M CHECKPOINT
PROTEIN SECRETION
INTERFERON ALPHA RESPONSE
8 - Naive CD4+ T cells
19 - CM CD4+ T cells TH1 CTLA4bright
4 - CD4+ T cells th22 CTLA4low PD1low
13 - EM CD4+ T cells ICOS+CTLA4+PD1+
12 - Naive CD8+ T cells
21 - EM CD8+ T cells CTLA4bright
11 - EM CD8+ CDTLA4+ 2B4+ T cells
1 - EMRA CD8+ CTLA4+ 2B4+ T cells
16 - Stem cell memory CD8+ T cells
30 - SCM CD8+ T cells TCRva72+
23 - CD8+ T cells TC2 activated CTLA4low
24 - Double negative th17 T cells CCR6+
29 - MAIT cells
27 - Regulatory T cells
20 - Class. monocytes CD11blow CD11clow
0 - Classical monocytes CD11bbright
31 - Classical monocytes CD39low
10 - Classical monocytes CD73+
22 - Class. monocytes CD73+ CD39+
3 - Classical monocytes IgM+ CD11bbright
35 - Classical monocytes IgM- CD11c+
2 - Classical monocytes KLRG1+
5 - Classical monocytes NKp46+
6 - Non classical monocytes
33 - Myeloïds macrophages
32 - Intermediate monocytes
28 - Dendritic cells
25 - Plasmacytoïd dendritic cells
9 - Naive B cells
26 - Non switched mem B cells
37 - Plasmocytes
15 - NK cells CD56bright CD16-
7 - NK cells CD56dim NKp30bright NKp46+
36 - NK cells CD56dim NKp46+ NKp30+
18 - NK cells CD56- NKp46low NKp30+
| NES |
1.5 2.0 2.5 3.0 3.5
NES
−2 0 2
in SR-GVHD
in SR-GVHD

Figure 4

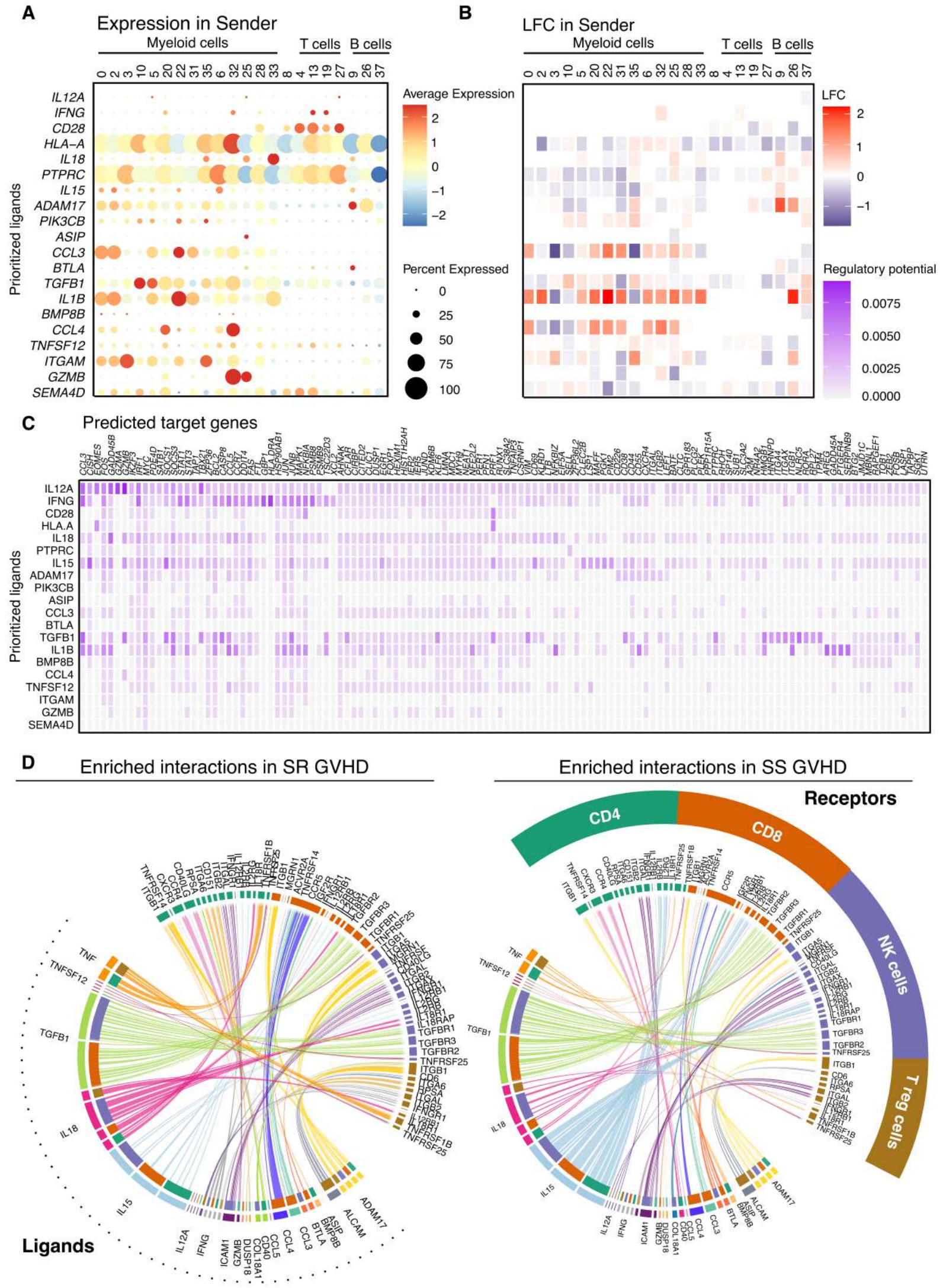
A
Expression in Sender
Myeloid cells
T cells
B cells
Prioritized ligands
IL12A
IFNG
CD28
HLA–A
IL18
PTPRC
IL15
ADAM17
PIK3CB
ASIP
CCL3
BTLA
TGFB1
IL1B
BMP8B
CCL4
TNFSF12
ITGAM
GZMB
SEMA4D
Average Expression
Percent Expressed
B
LFC in Sender
LFC
Regulatory potential
C
Predicted target genes
D
Enriched interactions in SR GVHD
Enriched interactions in SS GVHD
Receptors
CD4
CD8
NK cells
T reg cells
Ligands

Figure 5

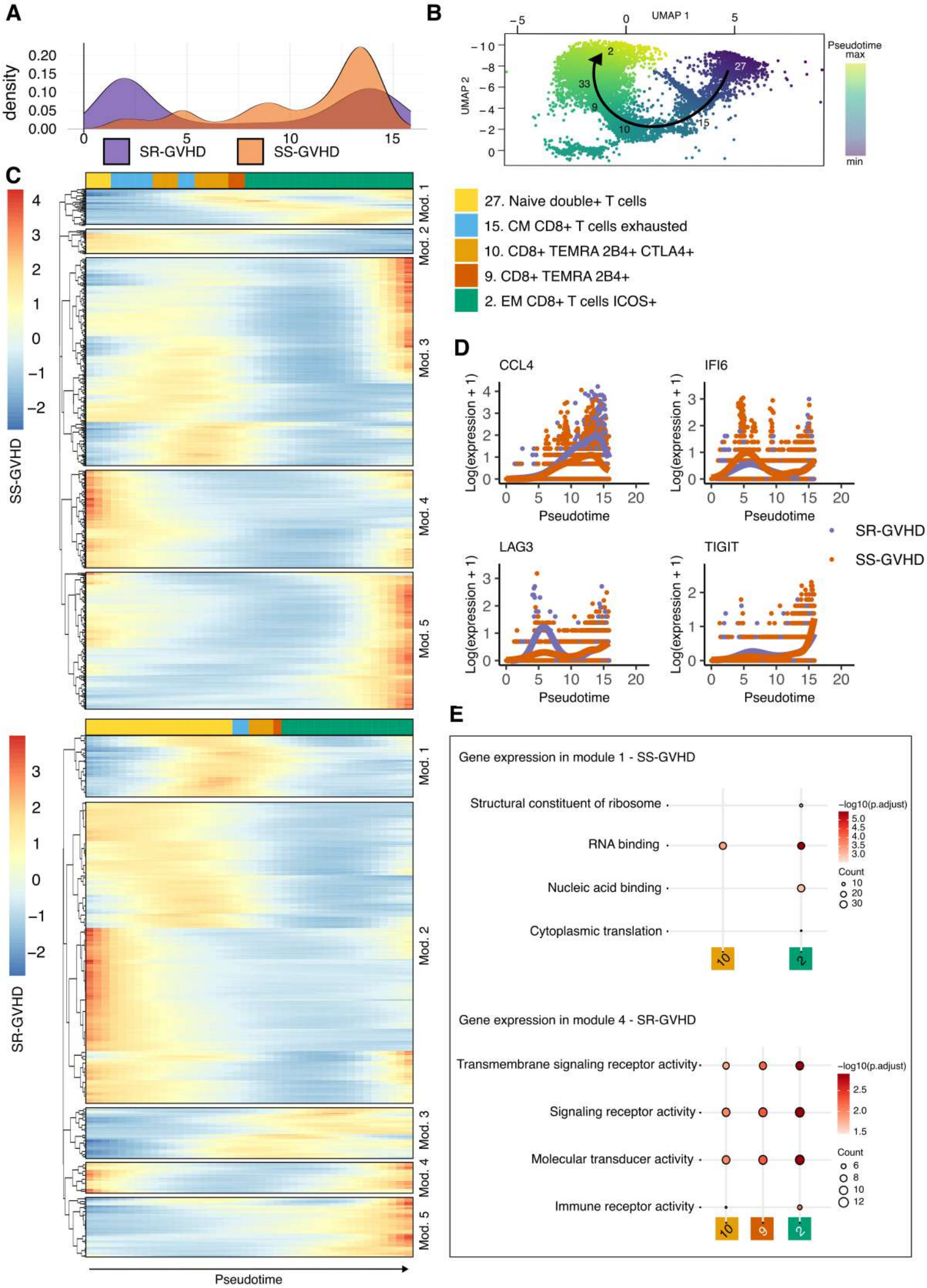
A
density
SR-GVHD
SS-GVHD
B
UMAP 1
UMAP 2
Pseudotime max
min
27. Naive double+ T cells
15. CM CD8+ T cells exhausted
10. CD8+ TEMRA 2B4+ CTLA4+
9. CD8+ TEMRA 2B4+
2. EM CD8+ T cells ICOS+
C
SS-GVHD
SR-GVHD
Mod. 1
Mod. 2
Mod. 3
Mod. 4
Mod. 5
Pseudotime
D
CCL4
IFI6
LAG3
TIGIT
Log(expression + 1)
Pseudotime
SR-GVHD
SS-GVHD
E
Gene expression in module 1 - SS-GVHD
Structural constituent of ribosome
RNA binding
Nucleic acid binding
Cytoplasmic translation
−log10(p.adjust)
Count
Gene expression in module 4 - SR-GVHD
Transmembrane signaling receptor activity
Signaling receptor activity
Molecular transducer activity
Immune receptor activity

Figure S1

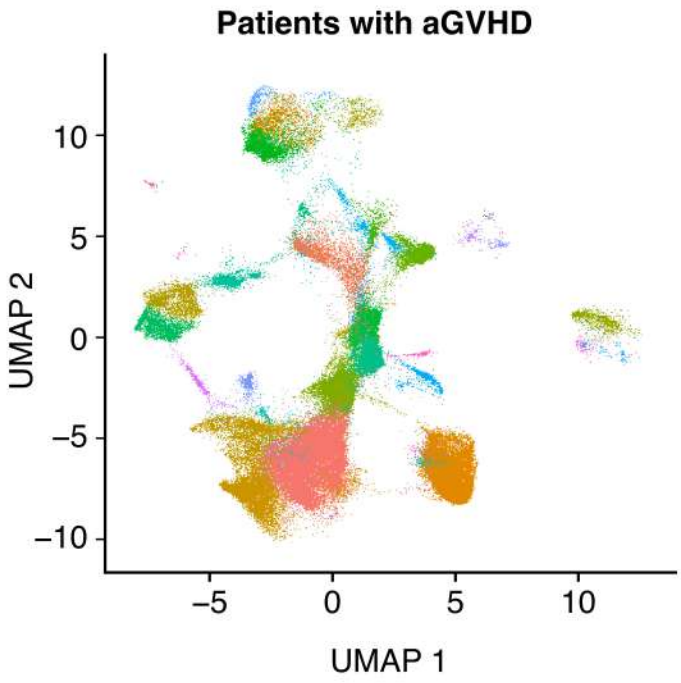

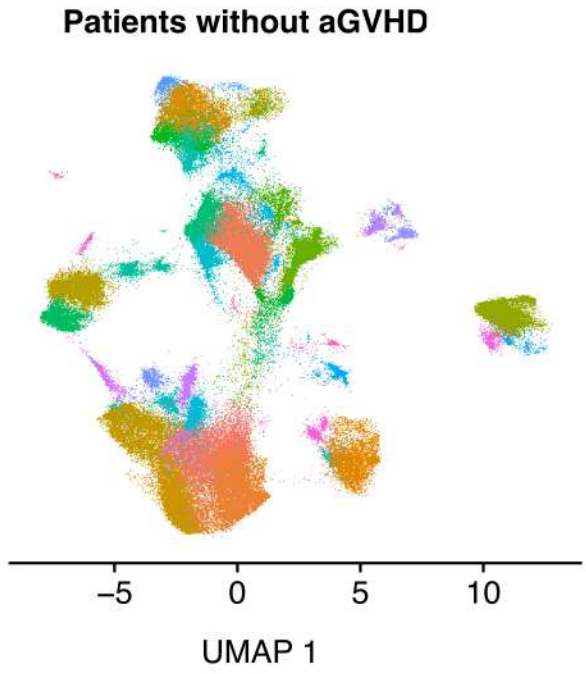

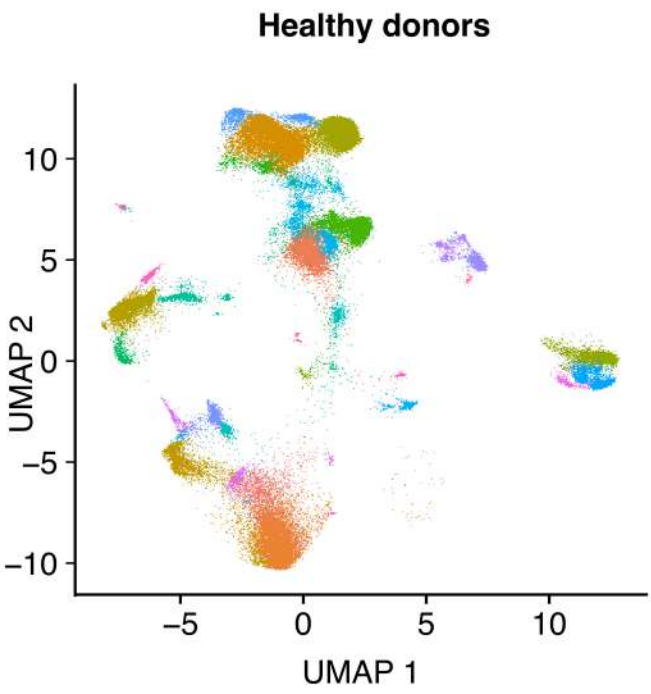

- 0 - Classical monocytes CD11b^{bright}
- 1 - EMRA CD8^{+} CTLA4^{+} 2B4^{+} T cells
- 2 - Classical monocytes KLRG1^{+}
- 3 - Classical monocytes IgM^{+} CD11b^{bright}
- 4 - CD4^{+} T cells th22 CTLA4^{low} PD1^{low}
- 5 - Classical monocytes NKp46^{+}
- 6 - Non classical monocytes
- 7 - NK cells CD56^{dim} NKp30^{bright} NKp46^{+}
- 8 - Naive CD4^{+} T cells
- 9 - Naive B cells
- 10 - Classical monocytes CD73^{+}
- 11 - EM CD8^{+} CTLA4^{+} 2B4^{+} T cells
- 12 - Naive CD8^{+} T cells
- 13 - EM CD4^{+} T cells ICOS^{+} CTLA4^{+} PD1^{+}
- 14 - Irrelevant population
- 15 - NK cells CD56^{bright} CD16^{-}
- 16 - Stem cell memory CD8^{+} T cells
- 17 - Irrelevant population
- 18 - NK cells CD56^{-} NKp46^{low} NKp30^{+}
- 19 - CM CD4^{+} T cells TH1 CTLA4^{bright}
- 20 - Class. monocytes CD11b^{low} CD11c^{low}
- 21 - EM CD8^{+} T cells CTLA4^{bright}
- 22 - Class. monocytes CD73^{+} CD39^{+}
- 23 - CD8^{+} T cells TC2 activated CTLA4^{low}
- 24 - Double negative th17 T cells CCR6^{+}
- 25 - Plasmacytoïd dendritic cells
- 26 - Non switched mem B cells
- 27 - Regulatory T cells
- 28 - Dendritic cells
- 29 - MAIT cells
- 30 - SCM CD8^{+} T cells TCRva72^{+}
- 31 - Classical monocytes CD39^{low}
- 32 - Intermediate monocytes
- 33 - Myeloïds macrophages
- 34 - Mature LB1
- 35 - Classical monocytes IgM^{+} CD11c^{+}
- 36 - NK cells CD56^{dim} NKp46^{+} NKp30^{+}
- 37 - Plasmocytes
- 17 - Irrelevant population
- 39 - Classical monocytes
- 40 - ILC2

Figure S2

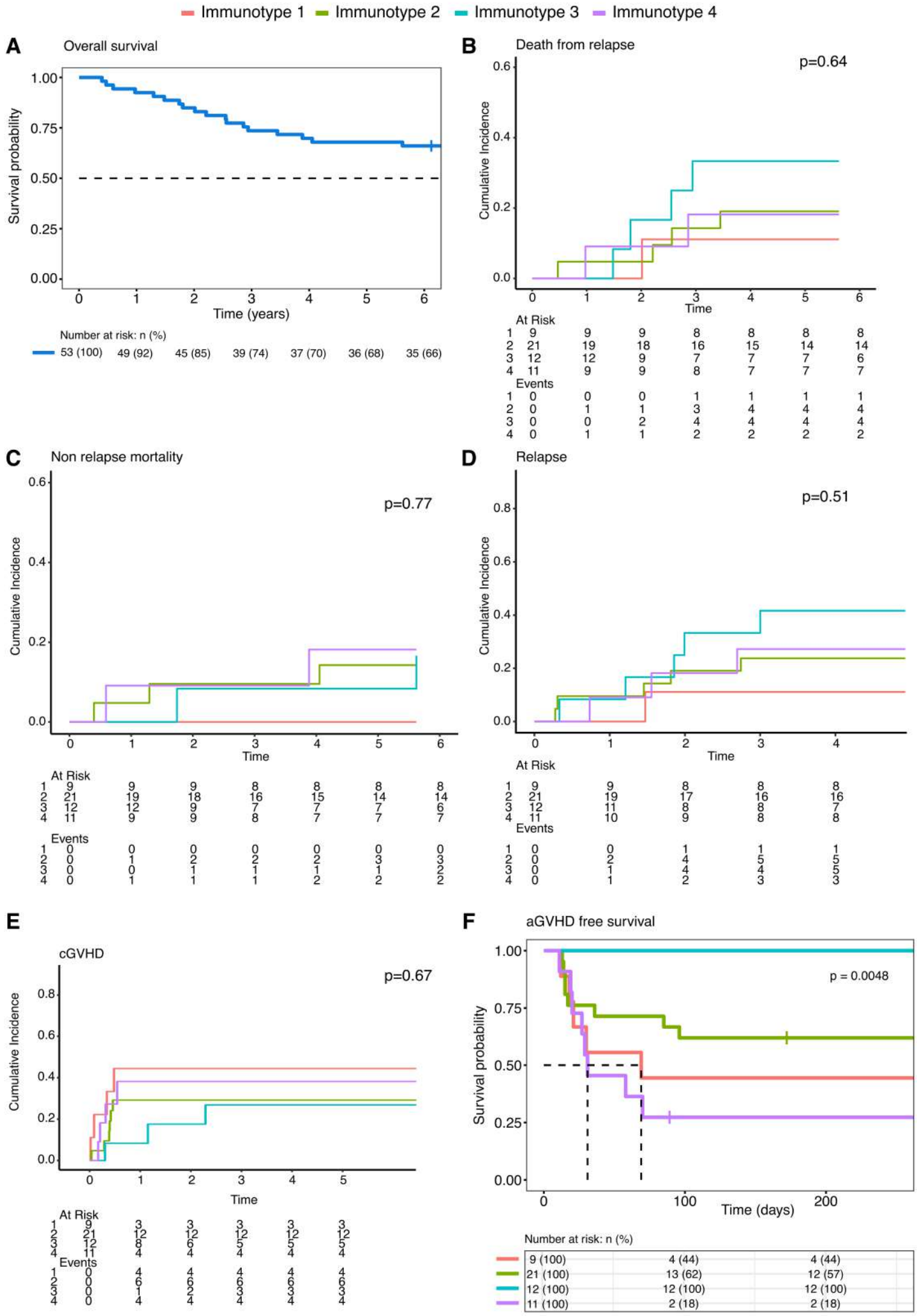
Immunotype 1
Immunotype 2
Immunotype 3
Immunotype 4
A
Overall survival
Survival probability
Time (years)
Number at risk: n (%)
53 (100) 49 (92) 45 (85) 39 (74) 37 (70) 36 (68) 35 (66)
B
Death from relapse
p=0.64
Cumulative Incidence
Time
At Risk
1 9 9 9 8 8 8 8
2 21 19 18 16 15 14 14
3 12 12 9 7 7 7 6
4 11 9 9 8 7 7 7
Events
1 0 0 0 1 1 1 1
2 0 1 1 3 4 4 4
3 0 0 2 4 4 4 4
4 0 1 1 2 2 2 2
C
Non relapse mortality
p=0.77
Cumulative Incidence
Time
At Risk
1 9 9 9 8 8 8 8
2 21 19 18 16 15 14 14
3 12 12 9 7 7 7 6
4 11 9 9 8 7 7 7
Events
1 0 0 0 0 0 0 0
2 0 1 2 2 2 3 3
3 0 0 1 1 1 1 2
4 0 1 1 1 2 2 2
D
Relapse
p=0.51
Cumulative Incidence
Time
At Risk
1 9 9 8 8 8
2 21 19 17 16 16
3 12 11 8 8 7
4 11 10 9 8 8
Events
1 0 0 1 1 1
2 0 2 4 5 5
3 0 1 4 4 5
4 0 1 2 3 3
E
cGVHD
p=0.67
Cumulative Incidence
Time
At Risk
1 9 3 3 3 3 3
2 21 12 12 12 12 12
3 12 8 6 5 5 5
4 11 4 4 4 4 4
Events
1 0 4 4 4 4 4
2 0 6 6 6 6 6
3 0 1 2 3 3 3
4 0 4 4 4 4 4
F
aGVHD free survival
p = 0.0048
Survival probability
Time (days)
Number at risk: n (%)
9 (100) 4 (44) 4 (44)
21 (100) 13 (62) 12 (57)
12 (100) 12 (100) 12 (100)
11 (100) 2 (18) 2 (18)

Figure S3

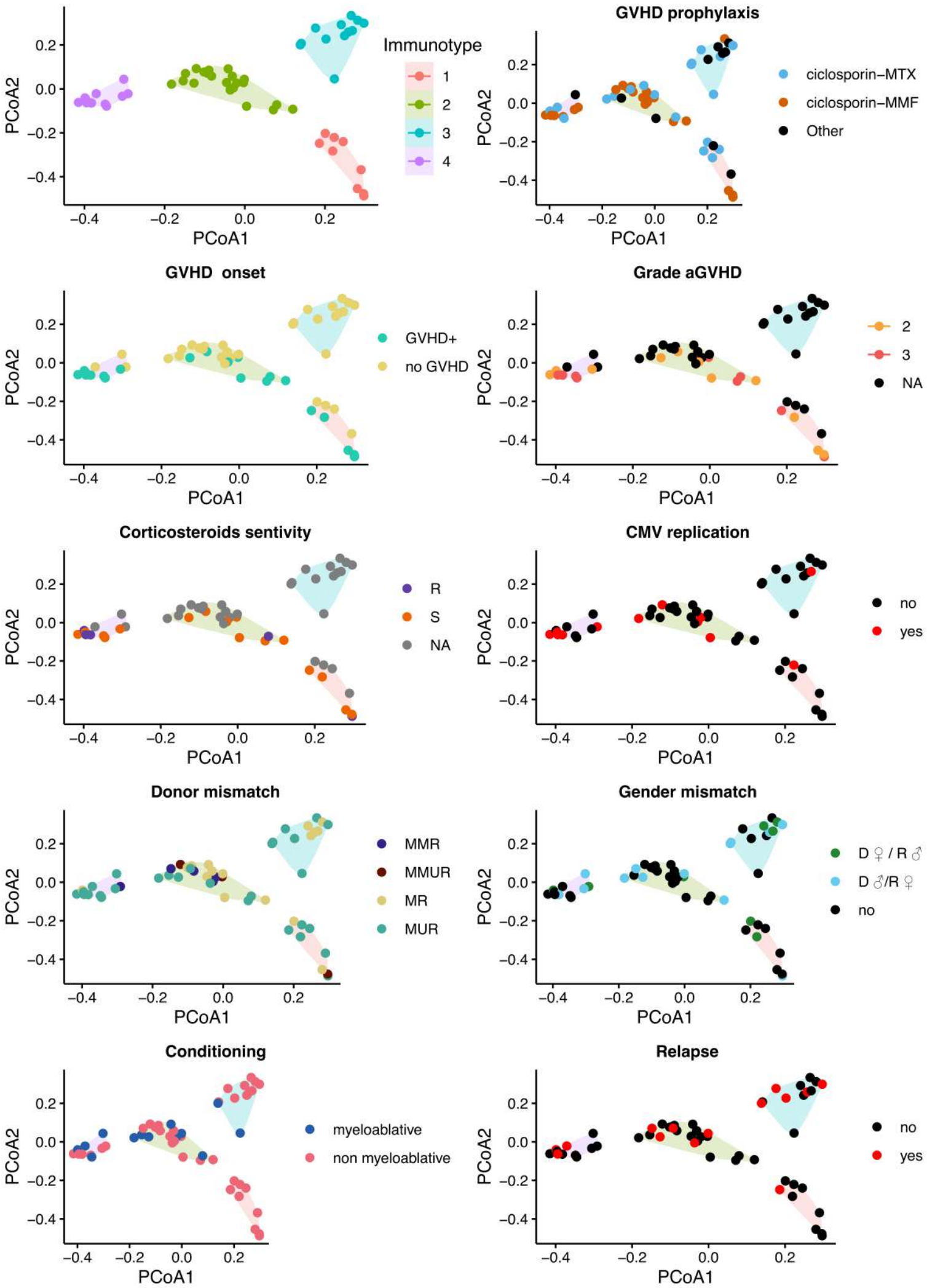
Immunotype
1
2
3
4
GVHD prophylaxis
ciclosporin−MTX
ciclosporin−MMF
Other
GVHD onset
GVHD+
no GVHD
Grade aGVHD
2
3
NA
Corticosteroids sentivity
R
S
NA
CMV replication
no
yes
Donor mismatch
MMR
MMUR
MR
MUR
Gender mismatch
D ♀ / R ♂
D ♂/R ♀
no
Conditioning
myeloablative
non myeloablative
Relapse
no
yes
PCoA1
PCoA2
−0.4
−0.2
0.0
0.2

FIgure S4

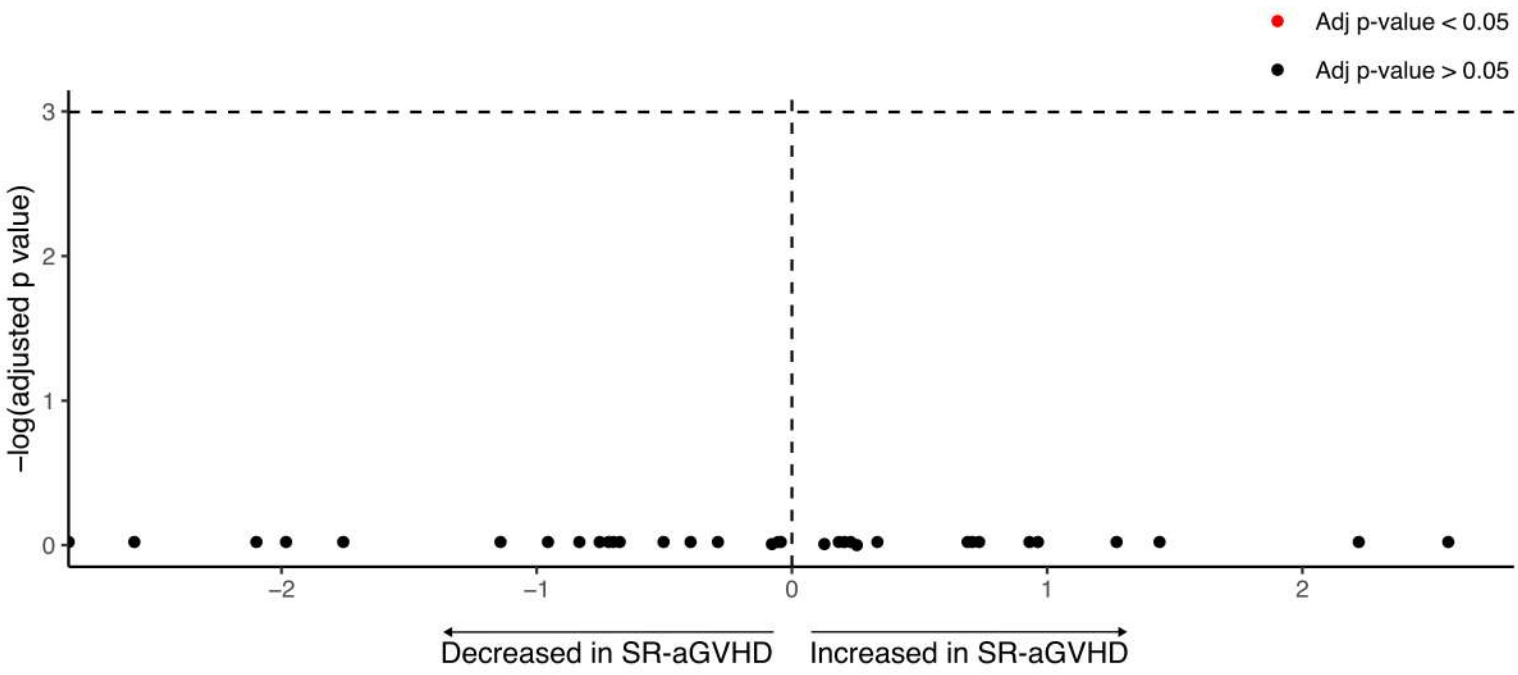
Adj p-value < 0.05
Adj p-value > 0.05
−log(adjusted p value)
3
2
1
0
−2
−1
0
1
2
Decreased in SR-aGVHD
Increased in SR-aGVHD

Figure S5

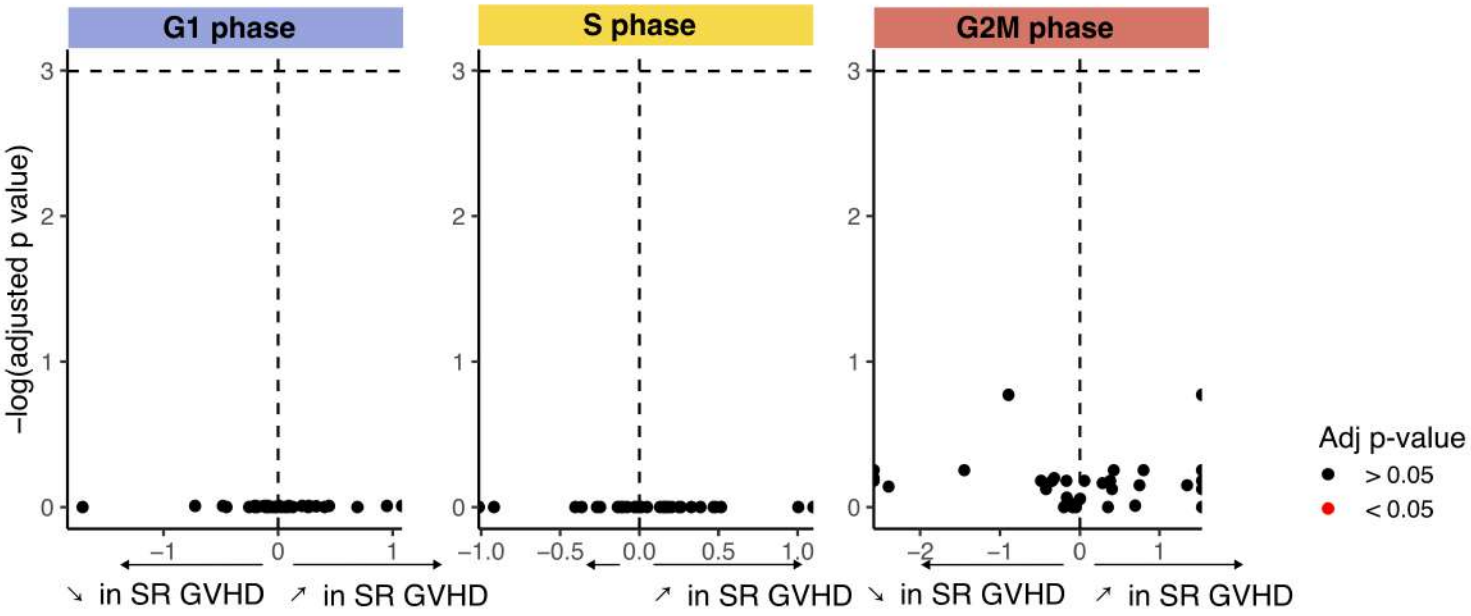
G1 phase
S phase
G2M phase
−log(adjusted p value)
3
2
1
0
−1
0
1
−1.0
−0.5
0.0
0.5
1.0
−2
↘ in SR GVHD
↗ in SR GVHD
↗ in SR GVHD
↘ in SR GVHD
↗ in SR GVHD
Adj p-value
> 0.05
< 0.05

Figure S6

OXIDATIVE_PHOSPHORYLATION
E2F_TARGETS
IL6_JAK_STAT3_SIGNALING
FATTY_ACID_METABOLISM
DNA_REPAIR
REACTIVE_OXYGEN_SPECIES_PATHWAY
MYC_TARGETS_V2
CHOLESTEROL_HOMEOSTASIS
XENOBIOTIC_METABOLISM
INTERFERON_ALPHA_RESPONSE
PEROXISOME
G2M_CHECKPOINT
ADIPOGENESIS
PI3K_AKT_MTOR_SIGNALING
INTERFERON_GAMMA_RESPONSE
MTORC1_SIGNALING
MYC_TARGETS_V1
COAGULATION
GLYCOLYSIS
COMPLEMENT
IL2_STAT5_SIGNALING
TGF_BETA_SIGNALING
APOPTOSIS
EPITHELIAL_MESENCHYMAL_TRANSITION
ALLOGRAFT_REJECTION
APICAL_JUNCTION
KRAS_SIGNALING_UP
INFLAMMATORY_RESPONSE
UV_RESPONSE_UP
HYPOXIA
P53_PATHWAY
UNFOLDED_PROTEIN_RESPONSE
KRAS_SIGNALING_DN
TNFA_SIGNALING_VIA_NFKB
ESTROGEN_RESPONSE_LATE
UV_RESPONSE_DN
MITOTIC_SPINDLE
HEME_METABOLISM
ANDROGEN_RESPONSE
ESTROGEN_RESPONSE_EARLY
Naive_CD4
CD4_CM_th1_CTLA4bright
CD4_CM_th22_CTLA4low_PD1low
CD4_EM_ICOS_PD1_CTLA4
naive_CD8
CD8_EM_CTLA4bright
CD8_EM_CTLA4pos_2B4pos
CD8_EMRA_CDTLA4pos_2B4pos
CD8_SCM
CD8_SCM_TCRva72pos
CD8_TC2_activated_CTLA4low
DN_th17_CCR6
ILC2
MAIT
Regulatory_T_cells
Clas_monocytes
clas_monocytes_CD11blow_CD11clow
clas_monocytes_CD11bright
clas_monocytes_CD39low
clas_monocytes_CD73pos
clas_monocytes_CD73pos_CD39pos
clas_monocytes_CD11bpos_CD11b_bright
clas_monocytes_IgMpos_CD11cpos
clas_monocytes_IgMpos_CD11b_bright
clas_monocytes_KLRG1pos
clas_monocytes_NLp46pos
Non_classical_monocytes
myeloids_Macrophages
inter_monocytes
myeloid_DC
pDC
mature_LB1
Naive_Bcells
Non_switched_IgM_memory_Bcells
Plasmocytes
NK_CD56br_CD16neg
NK_CD56dim_NKp30bright_NKp46pos
NK_CD56dim_NKp46pos_NKp30pos
NK_CD56neg_KID2DL1bright_NKp46low_NKp30pos
abs(NES)
2.0
2.5
3.0
3.5
NES
2
0
−2

Figure S7

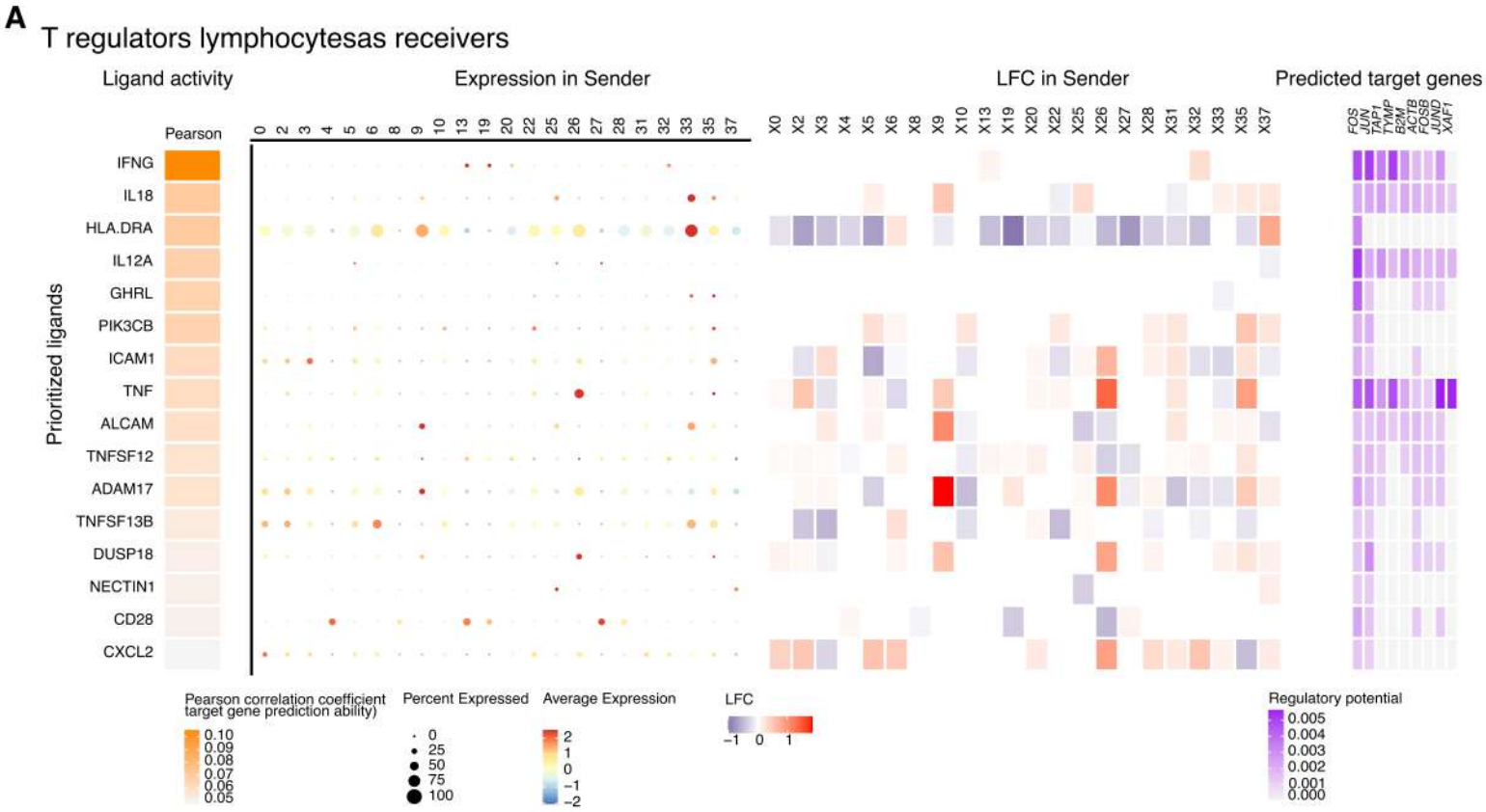
A
T regulators lymphocytesas receivers
Ligand activity
Expression in Sender
LFC in Sender
Predicted target genes
Pearson
Prioritized ligands
IFNG
IL18
HLA.DRA
IL12A
GHRL
PIK3CB
ICAM1
TNF
ALCAM
TNFSF12
ADAM17
TNFSF13B
DUSP18
NECTIN1
CD28
CXCL2
Pearson correlation coefficient target gene prediction ability)
Percent Expressed
Average Expression
LFC
Regulatory potential

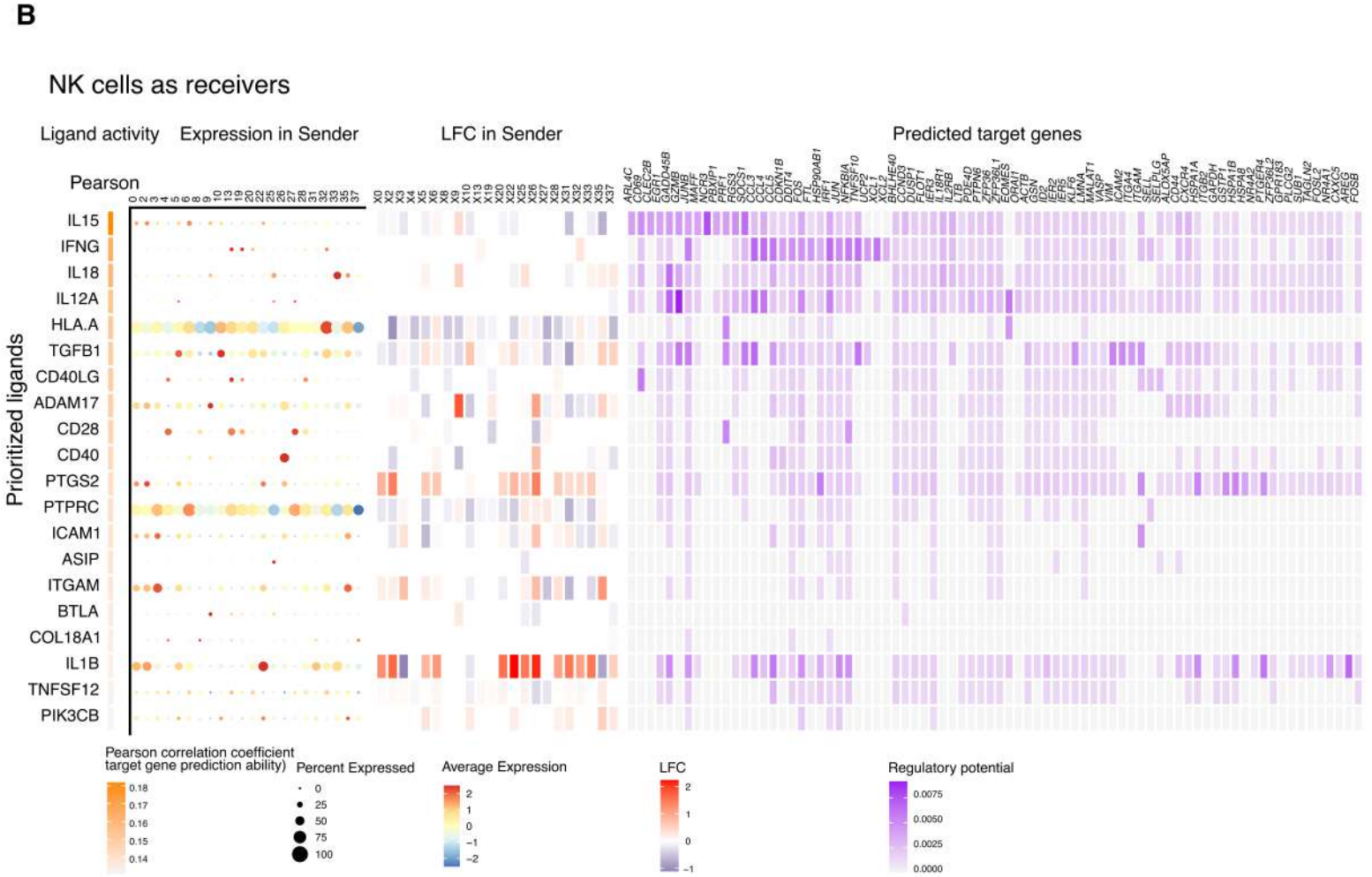
B
NK cells as receivers
Ligand activity
Expression in Sender
LFC in Sender
Predicted target genes
Pearson
Prioritized ligands
IL15
IFNG
IL18
IL12A
HLA.A
TGFB1
CD40LG
ADAM17
CD28
CD40
PTGS2
PTPRC
ICAM1
ASIP
ITGAM
BTLA
COL18A1
IL1B
TNFSF12
PIK3CB
Pearson correlation coefficient target gene prediction ability)
Percent Expressed
Average Expression
LFC
Regulatory potential

Figure S8

CD4⁺ T cells as receiver

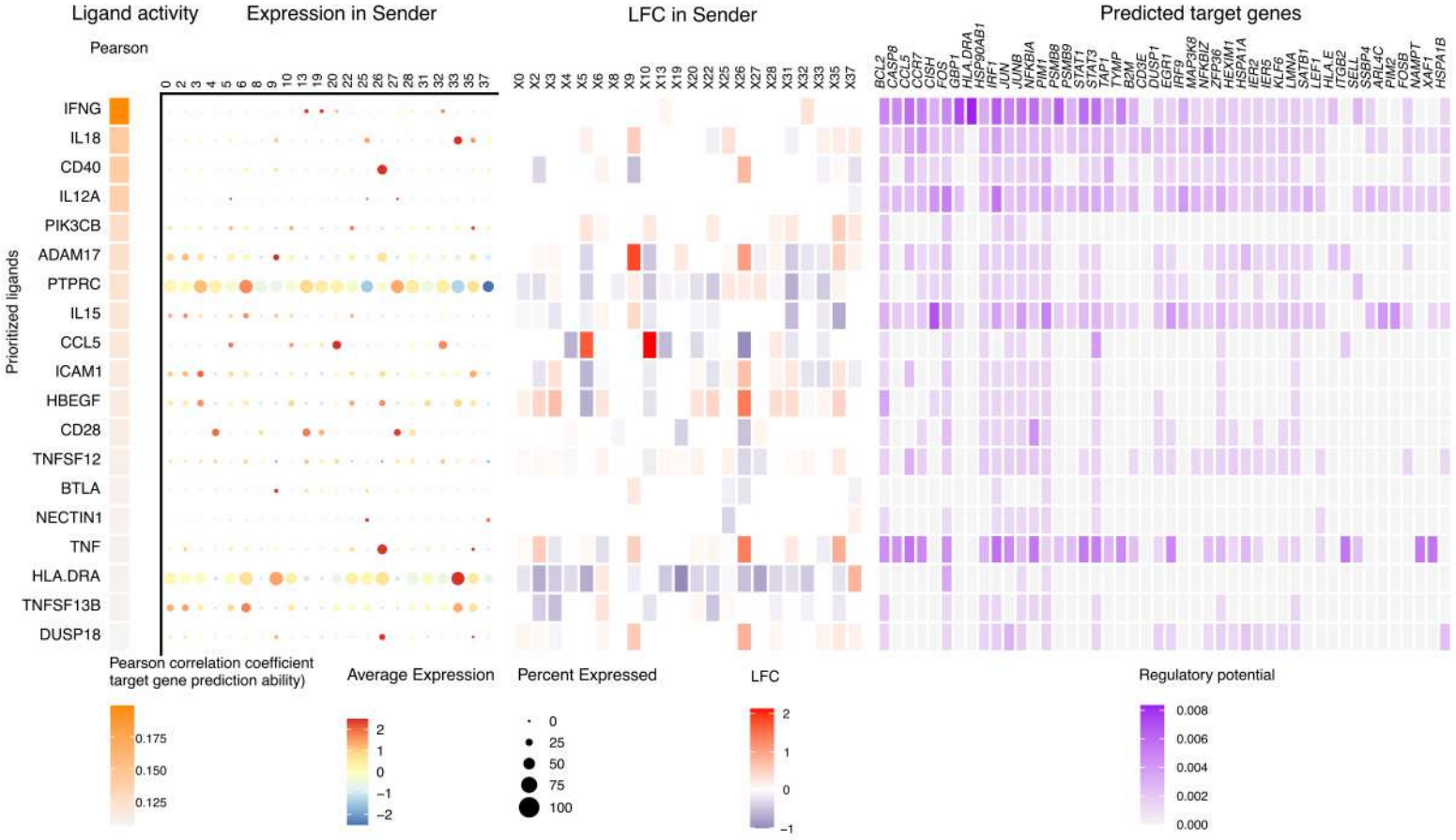

Double negative T cells as receiver

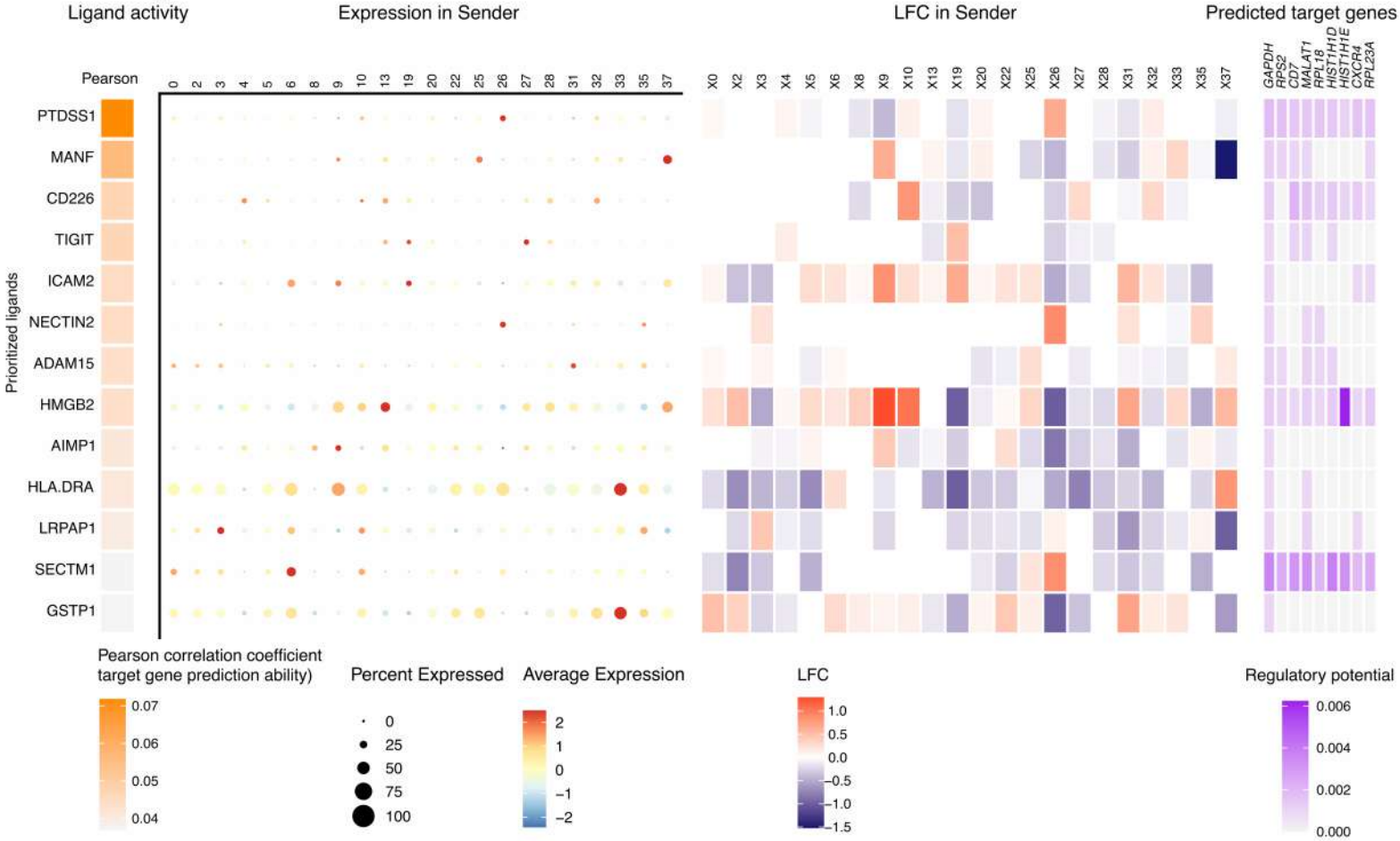

Figure S9

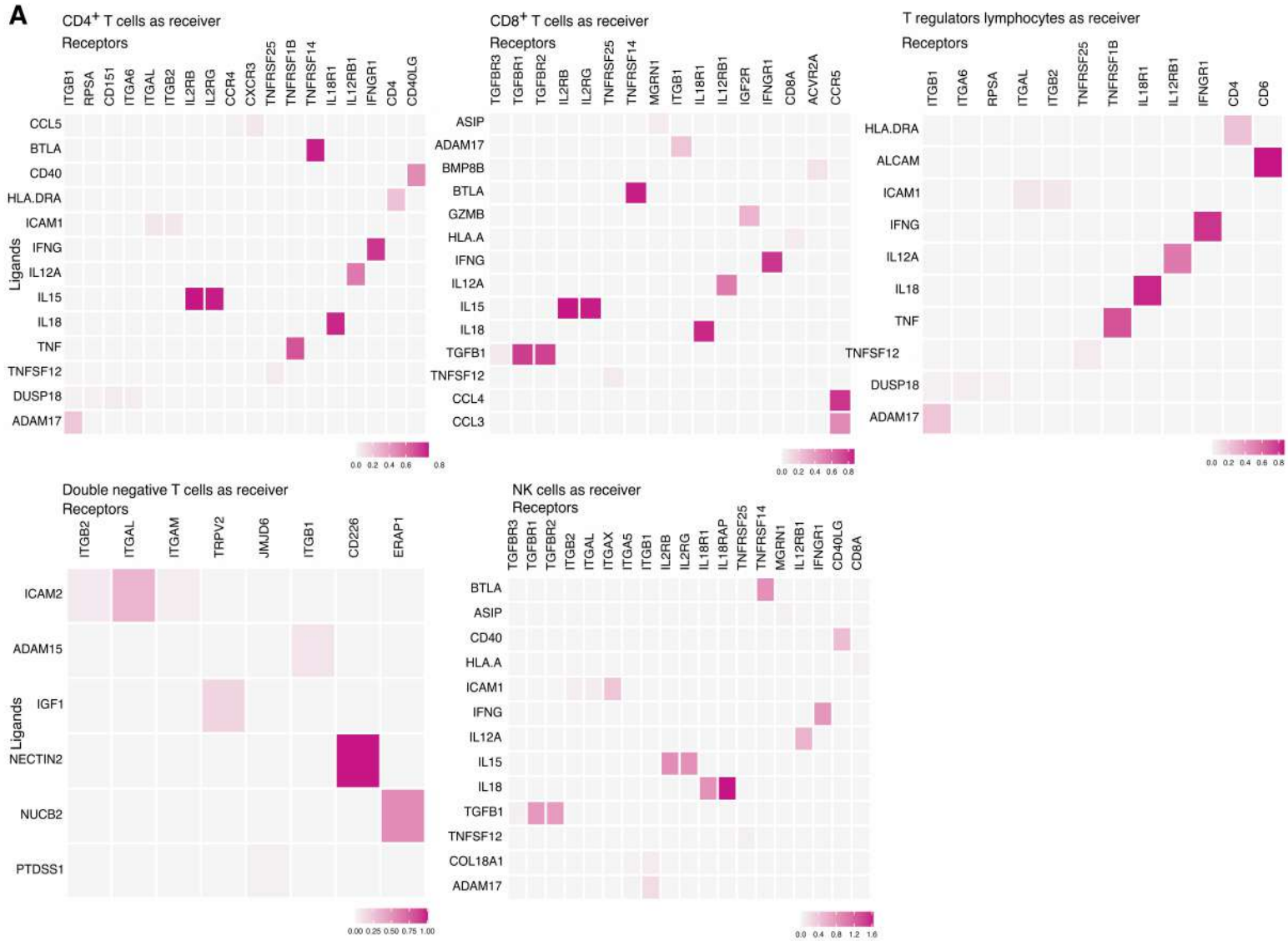
A
CD4+ T cells as receiver
Receptors
ITGB1 RPSA CD151 ITGA6 ITGAL ITGB2 IL2RB IL2RG CCR4 CXCR3 TNFRSF25 TNFRSF1B TNFRSF14 IL18R1 IL12RB1 IFNGR1 CD4 CD40LG
Ligands
CCL5 BTLA CD40 HLA.DRA ICAM1 IFNG IL12A IL15 IL18 TNF TNFSF12 DUSP18 ADAM17
CD8+ T cells as receiver
Receptors
TGFBR3 TGFBR1 TGFBR2 IL2RB IL2RG TNFRSF25 TNFRSF14 MGRN1 ITGB1 IL18R1 IL12RB1 IGF2R IFNGR1 CD8A ACVR2A CCR5
ASIP ADAM17 BMP8B BTLA GZMB HLA.A IFNG IL12A IL15 IL18 TGFB1 TNFSF12 CCL4 CCL3
T regulators lymphocytes as receiver
Receptors
ITGB1 ITGA6 RPSA ITGAL ITGB2 TNFRSF25 TNFRSF1B IL18R1 IL12RB1 IFNGR1 CD4 CD6
HLA.DRA ALCAM ICAM1 IFNG IL12A IL18 TNF TNFSF12 DUSP18 ADAM17
Double negative T cells as receiver
Receptors
ITGB2 ITGAL ITGAM TRPV2 JMJD6 ITGB1 CD226 ERAP1
Ligands
ICAM2 ADAM15 IGF1 NECTIN2 NUCB2 PTDSS1
NK cells as receiver
Receptors
TGFBR3 TGFBR1 TGFBR2 ITGB2 ITGAL ITGAX ITGA5 ITGB1 IL2RB IL2RG IL18R1 IL18RAP TNFRSF25 TNFRSF14 MGRN1 IL12RB1 IFNGR1 CD40LG CD8A
BTLA ASIP CD40 HLA.A ICAM1 IFNG IL12A IL15 IL18 TGFB1 TNFSF12 COL18A1 ADAM17

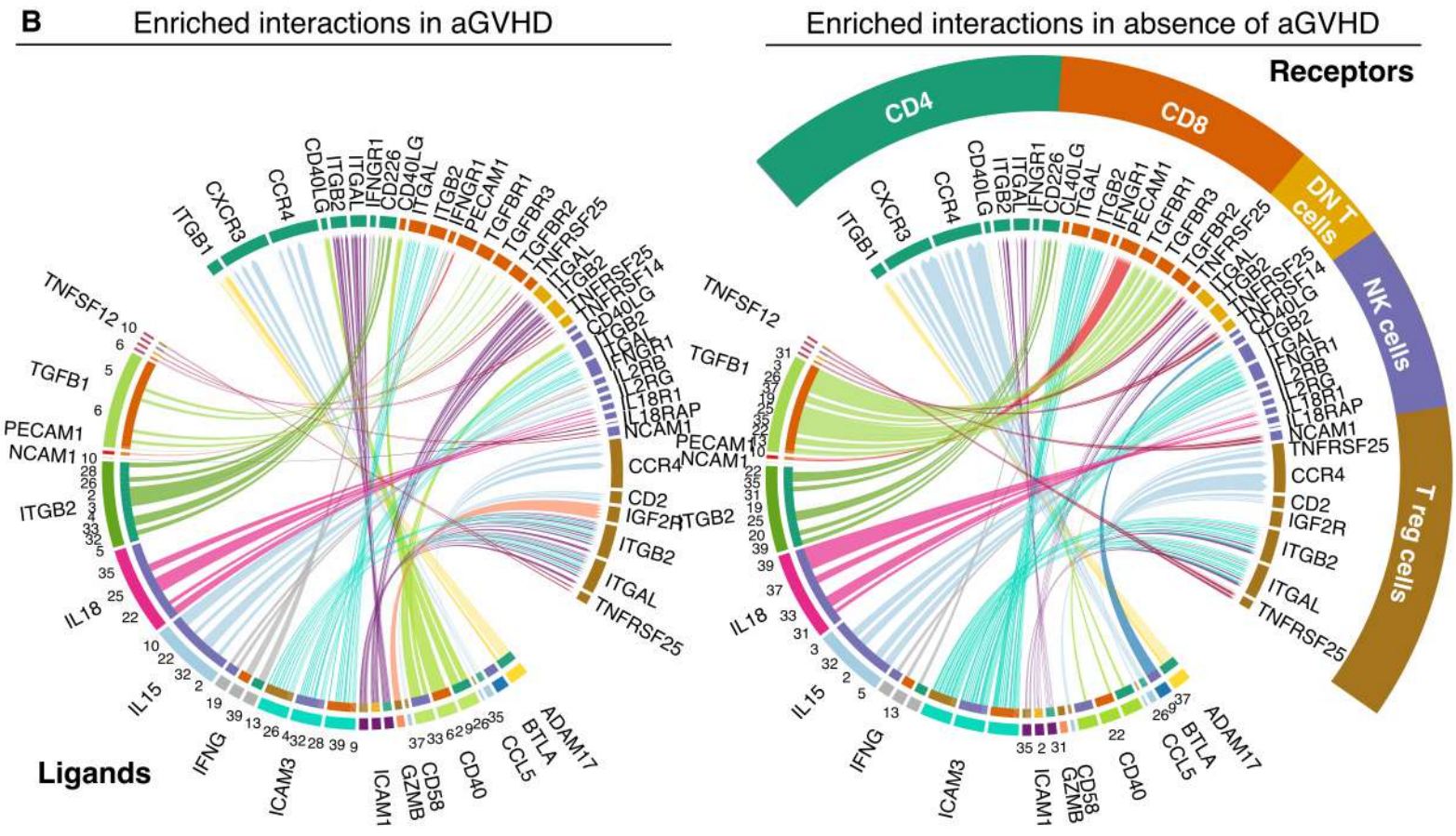
B
Enriched interactions in aGVHD
Enriched interactions in absence of aGVHD
Receptors
CD4
CD8
DN T cells
NK cells
T reg cells
Ligands
ITGB1 CXCR3 CCR4 CD40LG ITGB2 ITGAL IFNGR1 CD226 CD40LG ITGAL ITGB2 IFNGR1 PECAM1 TGFBR1 TGFBR3 TGFBR2 TNFRSF25 ITGAL ITGB2 TNFRSF25 TNFRSF14 CD40LG ITGB2 ITGAL IFNGR1 IL2RB IL2RG IL18R1 IL18RAP NCAM1 CCR4 CD2 IGF2R ITGB2 ITGAL TNFRSF25
TNFSF12 TGFB1 PECAM1 NCAM1 ITGB2 IL18 IL15 IFNG ICAM3 ICAM1 GZMB CD58 CD40 CCL5 BTLA ADAM17
TNFRSF25

Figure S10

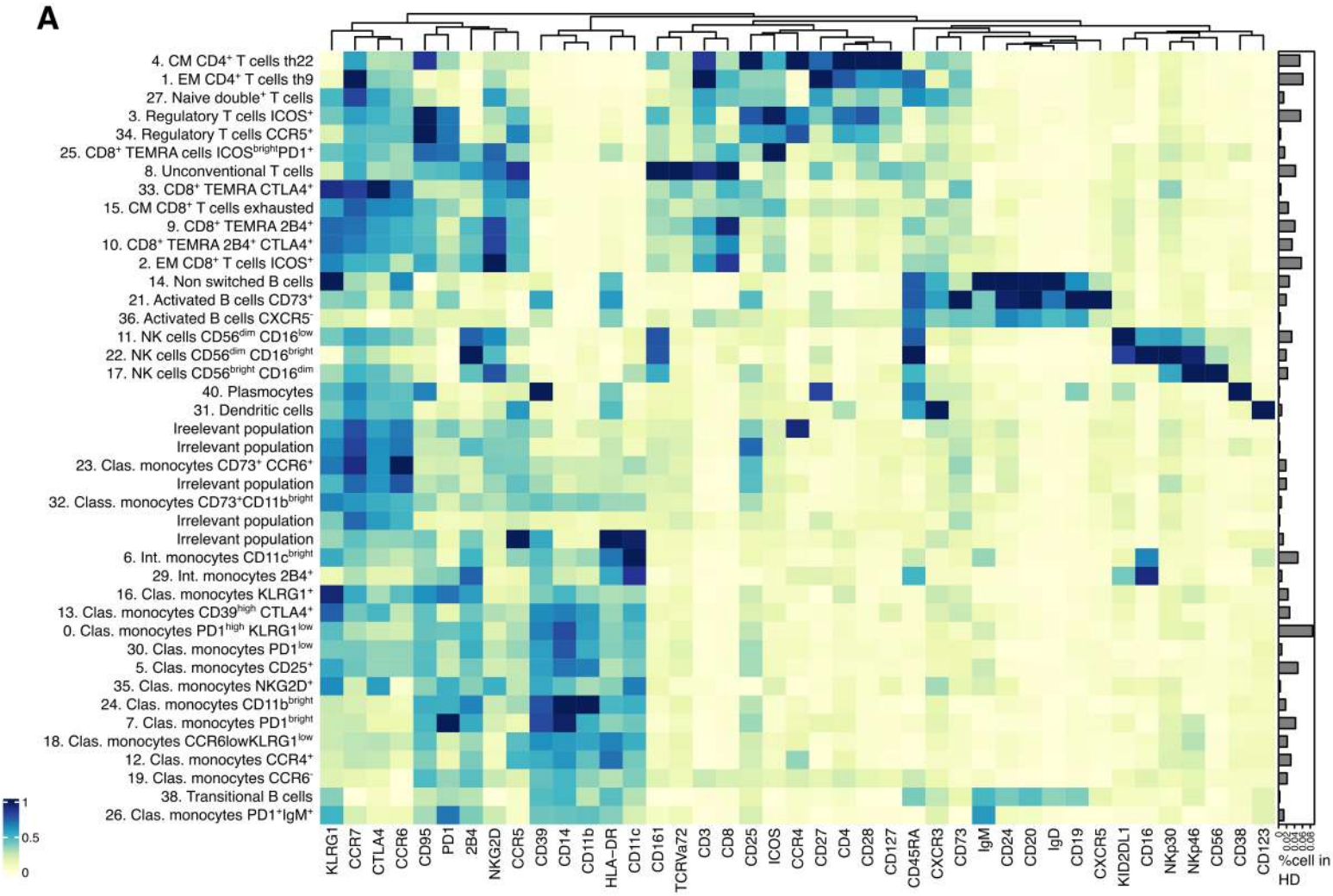
A
4. CM CD4+ T cells th22
1. EM CD4+ T cells th9
27. Naive double+ T cells
3. Regulatory T cells ICOS+
34. Regulatory T cells CCR5+
25. CD8+ TEMRA cells ICOSbrightPD1+
8. Unconventional T cells
33. CD8+ TEMRA CTLA4+
15. CM CD8+ T cells exhausted
9. CD8+ TEMRA 2B4+
10. CD8+ TEMRA 2B4+ CTLA4+
2. EM CD8+ T cells ICOS+
14. Non switched B cells
21. Activated B cells CD73+
36. Activated B cells CXCR5-
11. NK cells CD56dim CD16low
22. NK cells CD56dim CD16bright
17. NK cells CD56bright CD16dim
40. Plasmocytes
31. Dendritic cells
Ireelevant population
Irrelevant population
23. Clas. monocytes CD73+ CCR6+
Irrelevant population
32. Class. monocytes CD73+CD11bbright
Irrelevant population
Irrelevant population
6. Int. monocytes CD11cbright
29. Int. monocytes 2B4+
16. Clas. monocytes KLRG1+
13. Clas. monocytes CD39high CTLA4+
0. Clas. monocytes PD1high KLRG1low
30. Clas. monocytes PD1low
5. Clas. monocytes CD25+
35. Clas. monocytes NKG2D+
24. Clas. monocytes CD11bbright
7. Clas. monocytes PD1bright
18. Clas. monocytes CCR6lowKLRG1low
12. Clas. monocytes CCR4+
19. Clas. monocytes CCR6-
38. Transitional B cells
26. Clas. monocytes PD1+IgM+
KLRG1
CCR7
CTLA4
CCR6
CD95
PD1
2B4
NKG2D
CCR5
CD39
CD14
CD11b
HLA-DR
CD11c
CD161
TCRVa72
CD3
CD8
CD25
ICOS
CCR4
CD27
CD4
CD28
CD127
CD45RA
CXCR3
CD73
IgM
CD24
CD20
IgD
CD19
CXCR5
KID2DL1
CD16
NKp30
NKp46
CD56
CD38
CD123
%cell in HD
1
0.5
0

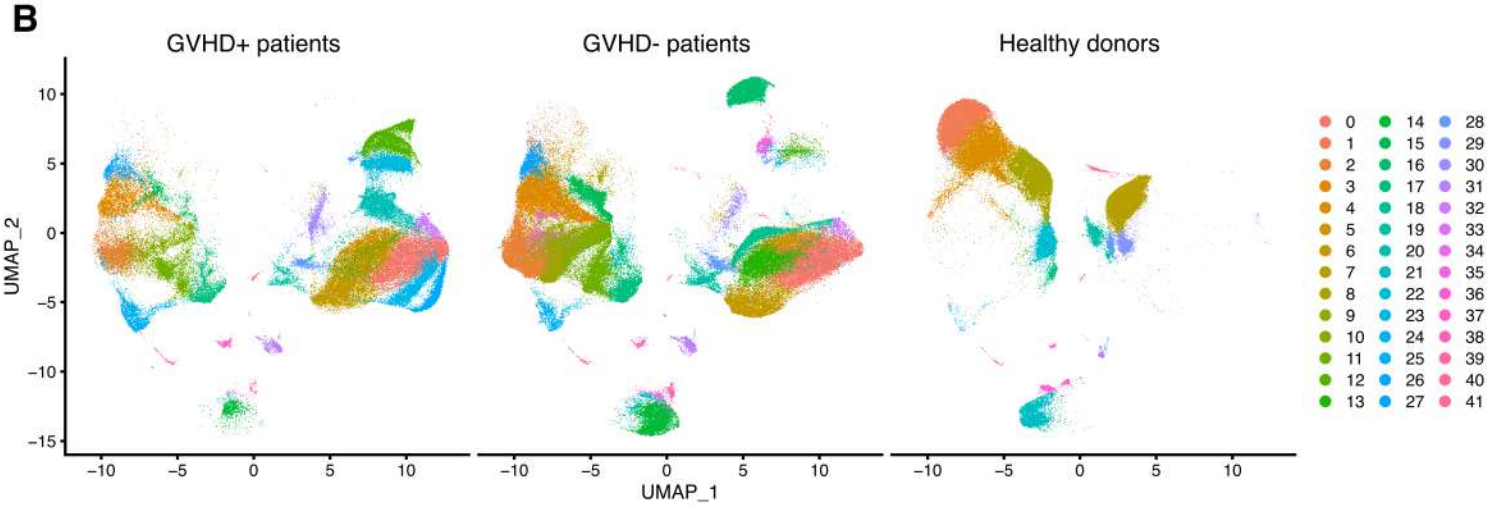
B
GVHD+ patients
GVHD- patients
Healthy donors
UMAP_2
UMAP_1
10
5
0
−5
−10
−15
0 1 2 3 4 5 6 7 8 9 10 11 12 13 14 15 16 17 18 19 20 21 22 23 24 25 26 27 28 29 30 31 32 33 34 35 36 37 38 39 40 41

Figure S11

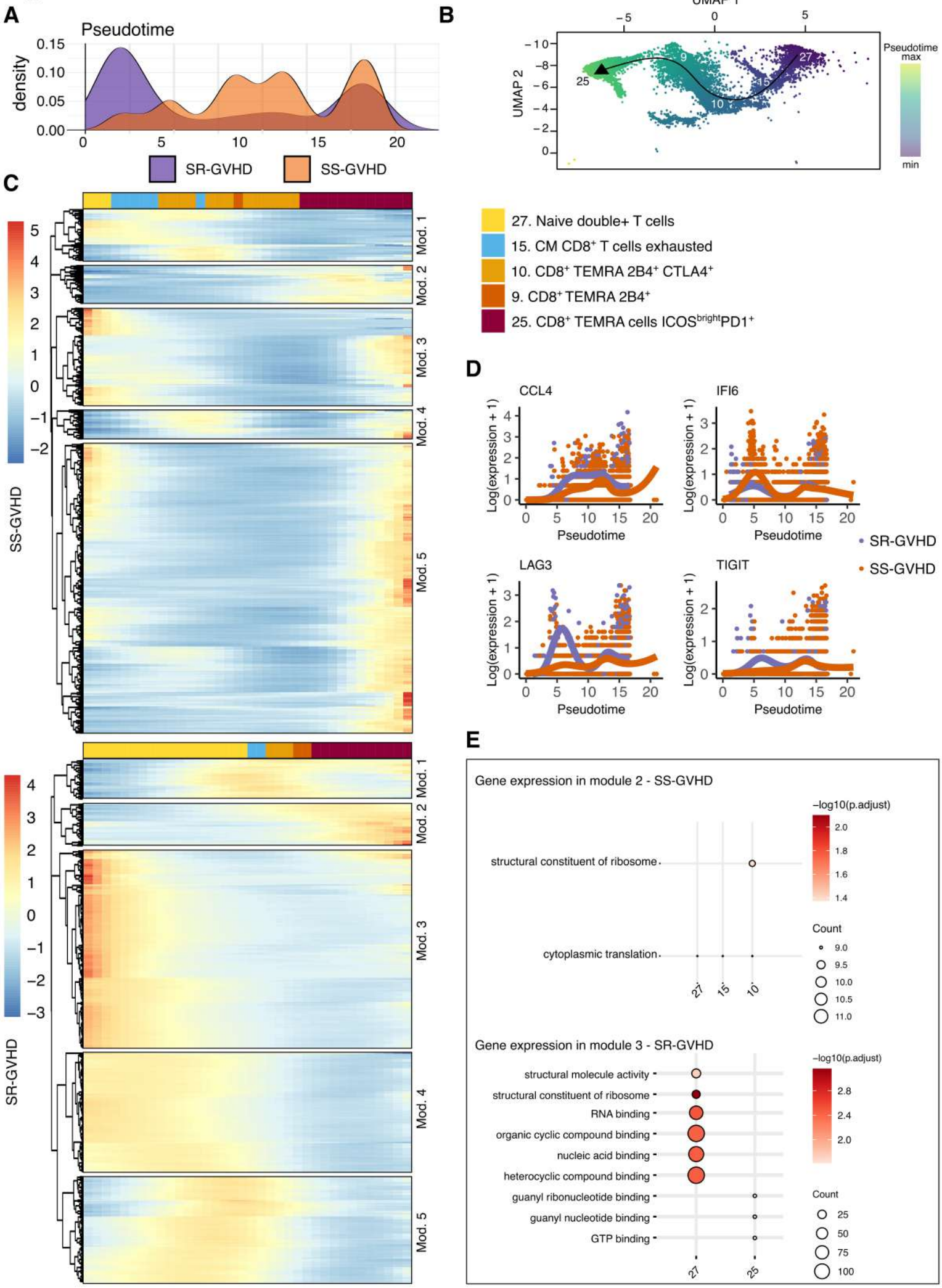
A
Pseudotime
density
SR-GVHD
SS-GVHD
B
UMAP 1
UMAP 2
Pseudotime max
min
27. Naive double+ T cells
15. CM CD8+ T cells exhausted
10. CD8+ TEMRA 2B4+ CTLA4+
9. CD8+ TEMRA 2B4+
25. CD8+ TEMRA cells ICOSbrightPD1+
C
SS-GVHD
SR-GVHD
Mod. 1
Mod. 2
Mod. 3
Mod. 4
Mod. 5
D
CCL4
IFI6
LAG3
TIGIT
Log(expression + 1)
Pseudotime
SR-GVHD
SS-GVHD
E
Gene expression in module 2 - SS-GVHD
structural constituent of ribosome
cytoplasmic translation
−log10(p.adjust)
Count
Gene expression in module 3 - SR-GVHD
structural molecule activity
structural constituent of ribosome
RNA binding
organic cyclic compound binding
nucleic acid binding
heterocyclic compound binding
guanyl ribonucleotide binding
guanyl nucleotide binding
GTP binding

Figure S12

Lineage 1 and SR-GVHD patients

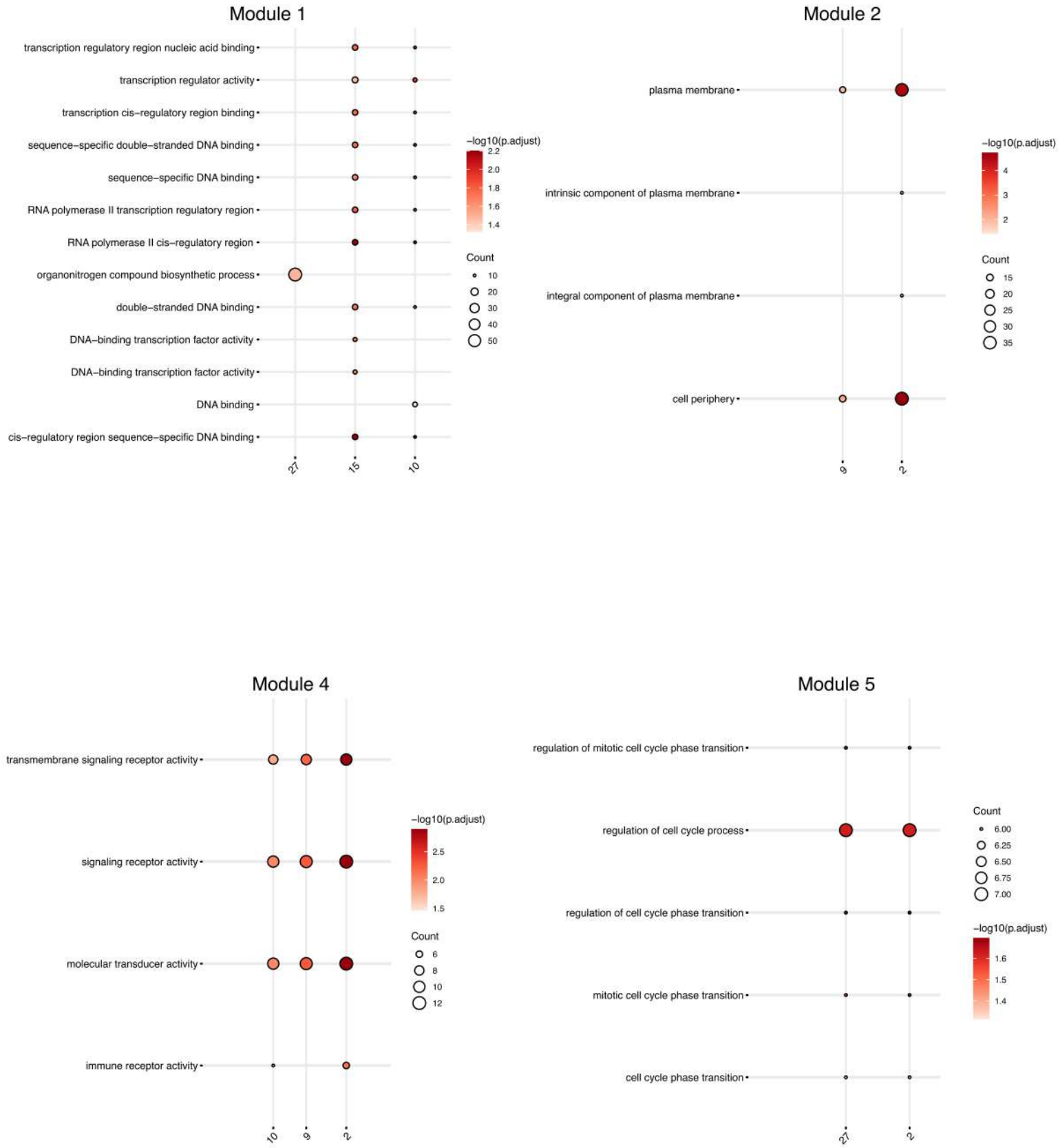

Figure S13

Lineage 1 and SS-GVHD patients

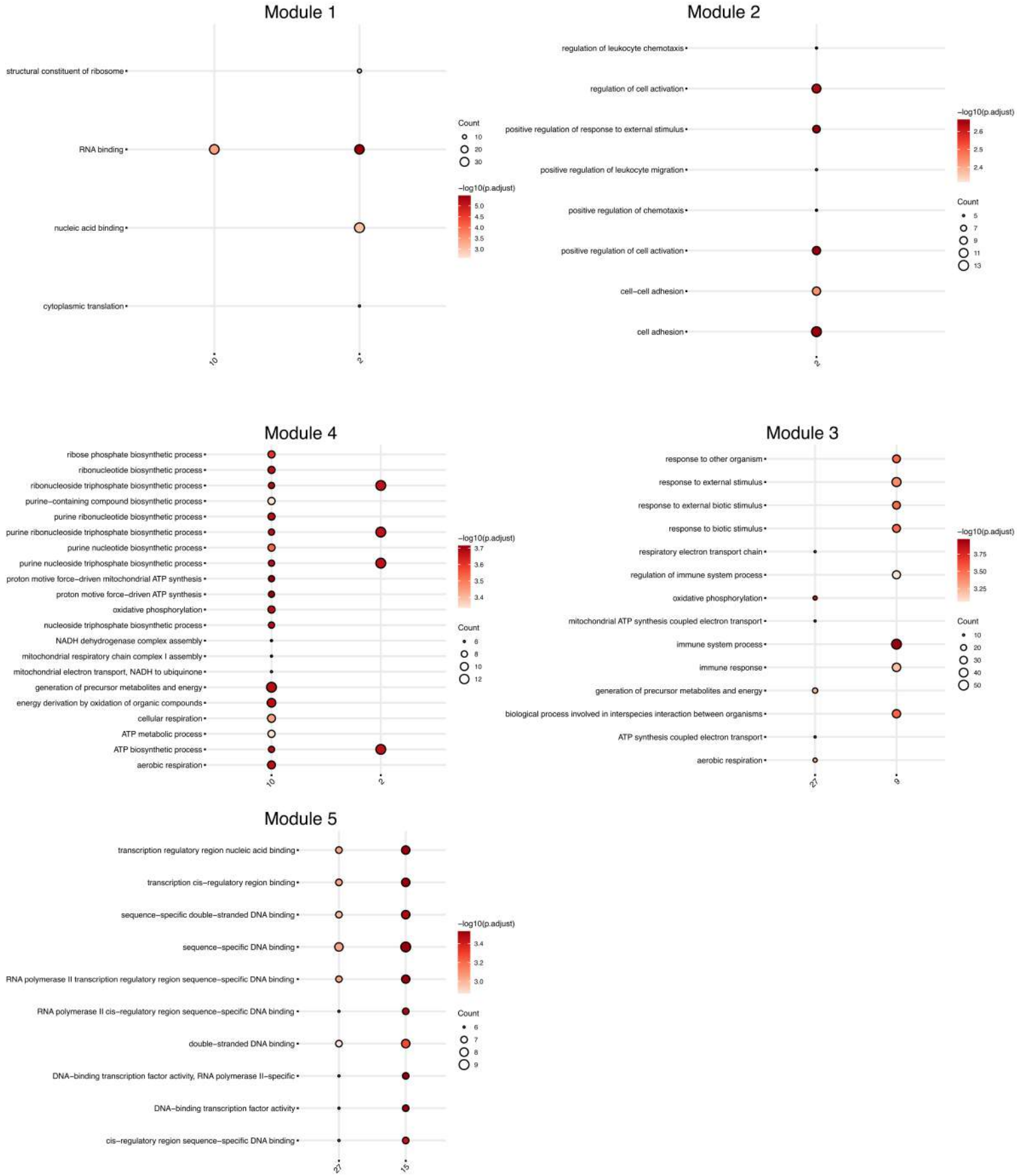

Figure S14

Lineage 2 and SR-GVHD patients

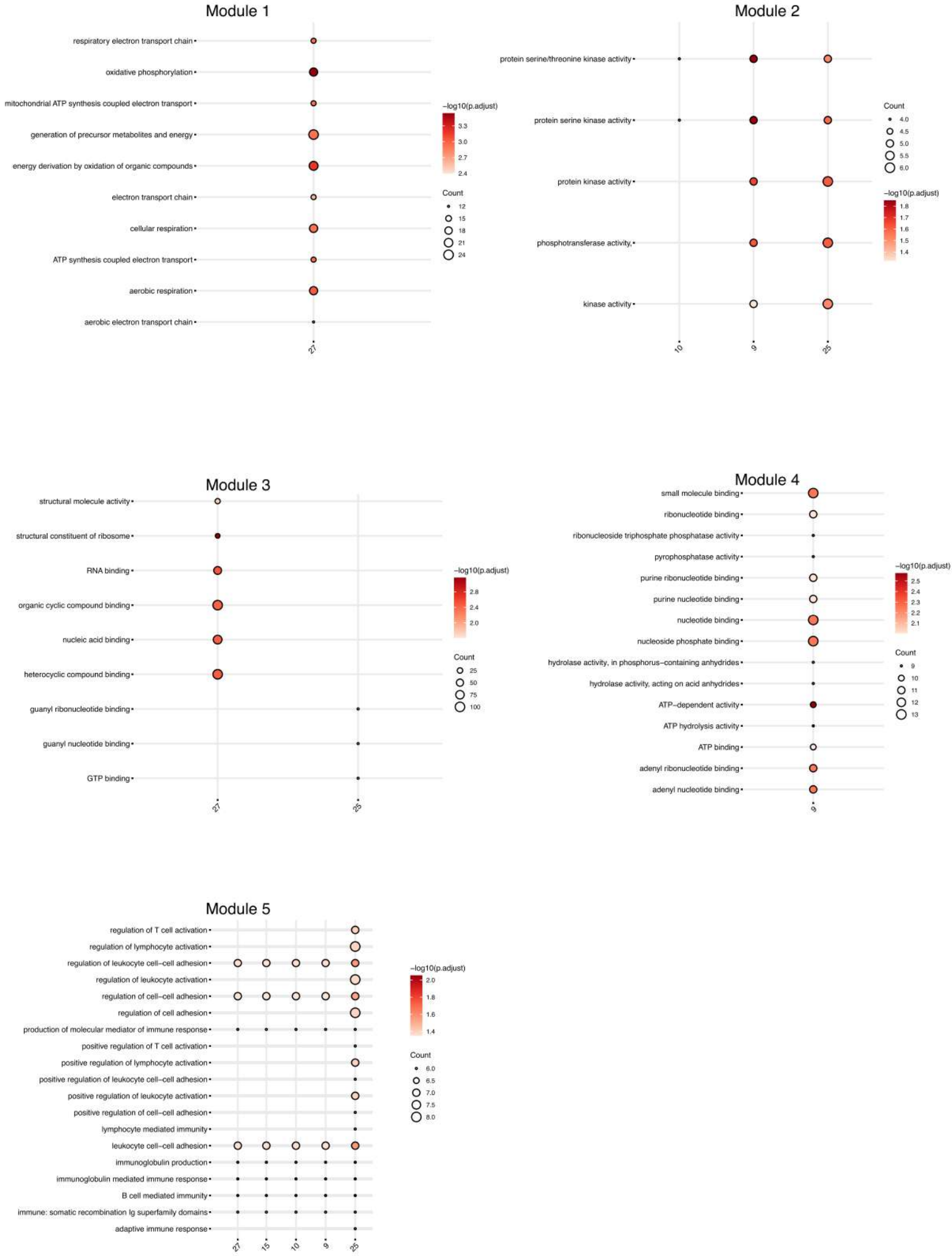

Figure S15
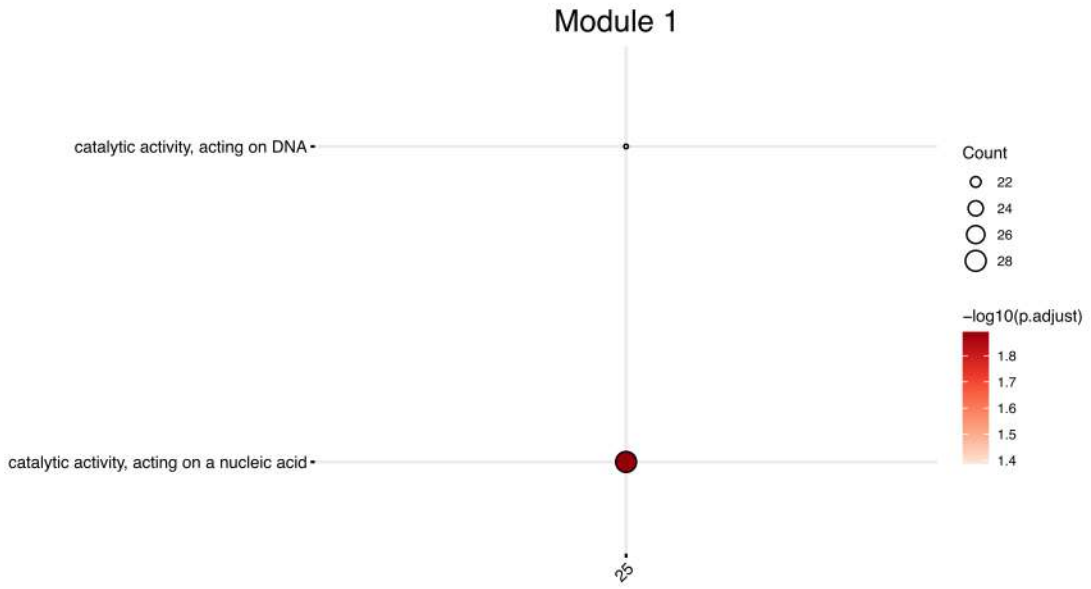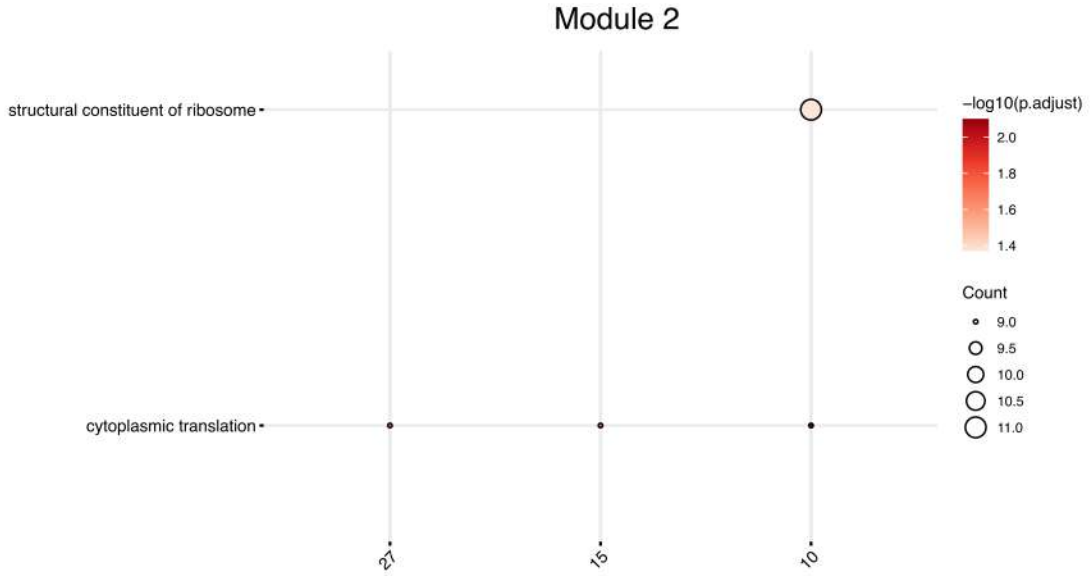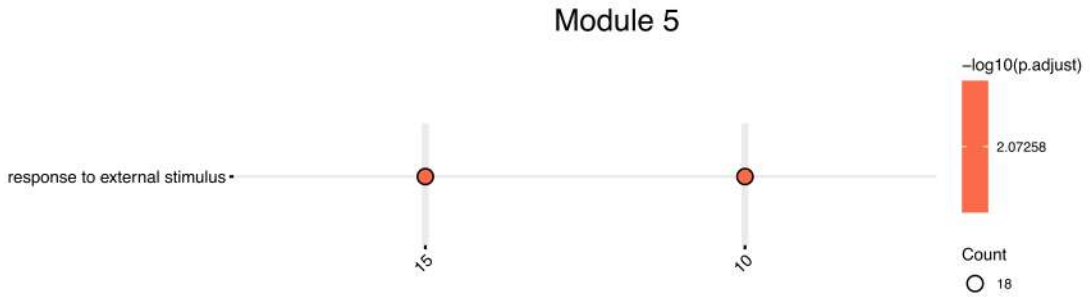
Lineage 2 and SS GVHD patients